ANATOMICAL AND PHYSIOLOGICAL STUDIES ON THE THYROID GLAND OF THE ALBINO RAT [1]

ADA R. HALL AND HELEN W. KAAN
Department of Zoology and Physiology, Wellesley College, Massachusetts

FOUR FIGURES

INTRODUCTION

In connection with some experiments on placental permeability and the effects on developing embryos of substances within the maternal blood stream, it became necessary to determine the exact course of development of the thyroid gland in rat embryos and to relate this to the onset of function. Following the preliminary report of the first series of experiments (Kaan and Hall, '37), two other series have considerably extended the available data.

According to Kull ('26), follicles containing colloid appear in the periphery of the gland in a rat embryo of 19 to 20 days gestation, and folliculation is complete by the twenty-second or twenty-third day, just before birth. Evidence for the onset of function of the rat thyroid is furnished by its ability to take up radio-active iodine at 18 to 19 days (Gorbman and Evans, '41). This occurs only in the peripheral region as shown by radio-autographs made from histological sections. Accumulation of iodine in the medullary region follows follicle formation there at 20 to 21 days. Kingsbury ('15) and Norris ('16) found the earliest appearance of colloid in the human thyroid at 2 to 3 months. They believe that the presence of

[1] Assisted by a grant from the American Academy of Arts and Sciences. We also wish to thank Paul Rummler for his assistance in the care of the animals.

THE ANATOMICAL RECORD, VOL. 84, NO. 3
NOVEMBER, 1942

colloid indicates that the gland is functional at this time. Lelkes ('33), however, did not find iodine in the human thyroid until the fourth month. Follicles appear in the thyroid of the pig at 50 to 55 days, when the embryos have a crown-rump length of 70 to 100 mm. (Moody, '10). Nevertheless, the functional activity, as determined by its effect on tadpole metamorphosis (Rumph and Smith, '26) appears only in the latter part of this period. Thyroids from 70 mm. embryos were unable to initiate metamorphic changes. The earliest indication of activity appeared in pigs of 90 mm., at which stage colloid was evident within the follicles. The recent work by Rankin ('41) corroborates the findings of Rumph and Smith. He obtained detectable amounts of thyroxine in embryos of 80 to 90 mm. (52 days). A marked increase in thyroxine accompanied the appearance of follicles and colloid within the gland of 120-mm. embryos (60 days). There is, thus, an obvious relationship between the appearance of follicles containing colloid and the onset of activity in the embryo thyroid.

Since various strains of rats differ considerably in postnatal growth, it is possible that a similar variation exists in the embryonic stages also. Consequently, development of the normal thyroid has been studied in the Wellesley strain of rats as a basis for the determination of functional activity. It was necessary, also, to measure the embryos at the various ages of gestation and calculate the size of the thyroids and the volume of colloid in each. To relate the degree of activity of the gland to the presence of two types of staining reaction in the colloid, sections were stained with Mallory's triple connective tissue stain. Results of this investigation have established (1) the age at which colloid first appears in the embryo and the age at which the two types of colloid can be differentiated, (2) the threshold of physiological activity of the glands as measured by tadpole metamorphosis, and (3) the relative potency of the colloid in glands containing so-called "active" colloid (blue staining) and those containing the storage type also (yellow or orange staining).

MATERIALS AND METHODS

The animals used in this investigation were albino rats inbred at Wellesley College for the last 11 years. The strain is characterized by large litters, little or no cannibalism, and gentle tractable animals. They tend to be definitely larger than the Wistar strain. This may be the result of diet. Dog or fox chow plus lettuce is used as stock diet, with the addition of paste food [2] during the last week of pregnancy and the 3 weeks of lactation.

The time at which mating occurred was determined by the vaginal smear method of Long and Evans ('22). The smears were taken between 9:00 and 10:00 A.M. and in most cases the sperm appeared in a fairly soft to liquid plug. In the second set of experiments the smears were made twice a day, 9:00 A.M. and 8:00 to 9:00 P.M. Nothing was gained by the evening smears as very few rats mated in the late afternoon. According to Blandau, Boling and Young ('39) the majority of rats come into heat between 5:00 and 11:00 P.M. which would favor early morning insemination. The age of the embryo was determined by allowing 24 hours for fertilization of the egg (Huber, '15) and then counting the age in days from that date. That is, if sperm were seen on the morning of one day, the count was begun on the morning of the following day, and the embryo considered 1 day old on the morning of the third day. By this method it was calculated that litters were born in the late afternoon of their twentieth day or, more often, on the morning of their twenty-first day. All embryos for study or injections were taken between 9:00 and 10:00 o'clock of the day for which a given age was required.

From each litter used for injection one embryo was preserved as a control to determine the size of the gland and condition of the colloid. The embryo was first weighed and measured (crown-rump) and the thyroid-parathyroid glands then fixed in aceto-formol-Mueller's fluid (Hewer, '29). In the first series, serial sections were stained by three methods,

[2] Whole milk powder, 25%; casein, 25%; wheat embryo, 20%; lard, 30%.

Erlich's haematoxylin and congo red, Erlich's and Biebrich scarlet, and Mallory's triple stain. In the second series only Mallory's stain was used, as this gave the best differentiation of the cells and of the colloid of both types.

The remainder of each litter was then weighed and the average weight of the individuals determined. Each embryo was measured individually. The thyroid was dissected out aseptically and placed in a drop of sterile Ringer's solution in a tiny mortar. This mortar was made by grinding wet carborundum in a small stender dish with a heavy glass rod flat on the end. These ground surfaces gave enough friction to completely macerate the embryonic glands. After grinding the glands from a whole litter or more in 1 or 2 drops of saline, this was taken up in a Luer syringe (1 cc. calibrated in 100ths). Another drop of saline was placed in the dish, ground and taken up. The dish was rinsed drop by drop until the syringe contained fluid enough to allow .05 cc. for each tadpole to be injected. The needle was then placed on the syringe, a bubble of air drawn in and the whole contents of the syringe mixed thoroughly. Injections into tadpoles were made intraperitoneally. All embryonic material was collected and the tadpoles injected in the fall and early winter (Rankin, '41).

Several entire litters of embryos of various ages were preserved and sectioned to determine the variation among litter mates. In such cases, each embryo was measured and weighed before dissecting the thyroid-parathyroid apparatus for preservation.

To determine the size of the gland, serial sections (10 μ thick) were projected and drawn at a magnification of × 69. Every fourth section in the series was drawn. The area of these drawings was then measured with a planimeter and the sum total determined for the whole thyroid. The area of the original gland was computed as the magnified area divided by the square of the magnification. This represented the area of one-fourth of the original gland, and the volume was calculated as the area multiplied by four times the thickness of the original sections in millimeters. This gave the absolute

volume of the entire gland in cubic millimeters. The volume of the thyroid was also calculated in cubic millimeters per 100 sq.cm. of body surface, since many workers consider body surface a better criterion than weight in judging an animal's metabolism. For such calculations the following formula was used.

$$S = 9.1\ W^{2/3}$$

where S equals surface in square centimeters, W equals weight in grams.

For calculating the colloid as a per cent of the total gland, a different method was used. The colloid masses, even at a magnification of × 710, were in many cases too small to be determined accurately by the planimeter. Consequently camera lucida drawings of most of the area of the gland at each of ten levels were made on firm paper and the whole drawing dried and weighed. The outline of the colloid was then cut out with fine scissors and the remaining paper dried and weighed. The difference between these weights was the colloid weight. From the total and the colloid weights the per cent of colloid was determined.

The tadpoles used for testing the physiological activity of the embryonic glands at various ages were those of Rana clamitans, the large green frog. These tadpoles were 51 to 85 mm. in length and had small undifferentiated limb buds. In the preliminary experiments the tadpoles were kept in running lake water at a temperature of 14°C. For series A and B a heat regulator was used and the temperature ranged from 18° to 22°C. The tadpoles were placed by twos in finger bowls with galvanized wire covers and sunk in a trough of running water of the desired temperature. No feeding was attempted for the 2-weeks' experimental period. For series C the finger bowls were set on the table in a room of the desired temperature and the water changed daily. This was the most satisfactory procedure for keeping a constant temperature.

Measurements of total length, tail length and leg length were recorded at weekly intervals before and after the in-

jection of rat thyroids. The body and tail measurements were made with calipers as the animal lay in a narrow wax dish of water. Leg length was taken as the animal lay out of water on a wet glass surface under a reading glass. No ice or anesthesia was used.

TABLE 1

Averages of the measurements of foetal albino rats.[1]

FOETAL AGE	NO. RATS	WEIGHT	LENGTH	BODY SURF.	THYROID VOL.	CU.MM. THY. PER 100 SQ.CM. B. SURF	COLLIOD		
							No. rats	% of total	Cu.mm. per gland
days		*gm.*	*cm.*	*sq.cm.*	*cu.mm.*				
15	5	.456± .0044	1.72± .0062	5.33	.0481± .0031	.893			
16	7	.845± .0168	2.08± .0243	8.12	.1297± .0042	1.590			
17	7	1.286± .0175	2.52± .0166	10.75	.2718± .0571	2.521	2	.75	.0020
18	14	1.939± .0310	2.95± .0202	14.13	.4436± .0118	3.130	6	2.72	.0121
19	16	3.166± .0835	3.59± .0335	19.56	.5419± .0109	2.778	5	5.95	.0322
20	13	4.569± .0447	3.92± .0200	25.03	.5979± .0109	2.396	5	9.39	.0561
21 just born	6	4.996± .0936	4.19± .1590	26.46	.5707± .0126	2.156	5	10.21	.0583
22	9	5.096± .0646	4.32± .1030	26.93	.5315± .0198	1.967	5	13.04	.0693

[1] Data for individual animals are available and may be obtained by writing the authors.

RESULTS AND DISCUSSION

The actual measurements of all fetal, just-born, and 1-day-old rats are recorded in table 1. In figure 1 both body length and thyroid size have been plotted against body weight. It is noticeable that weight is more variable than length at any

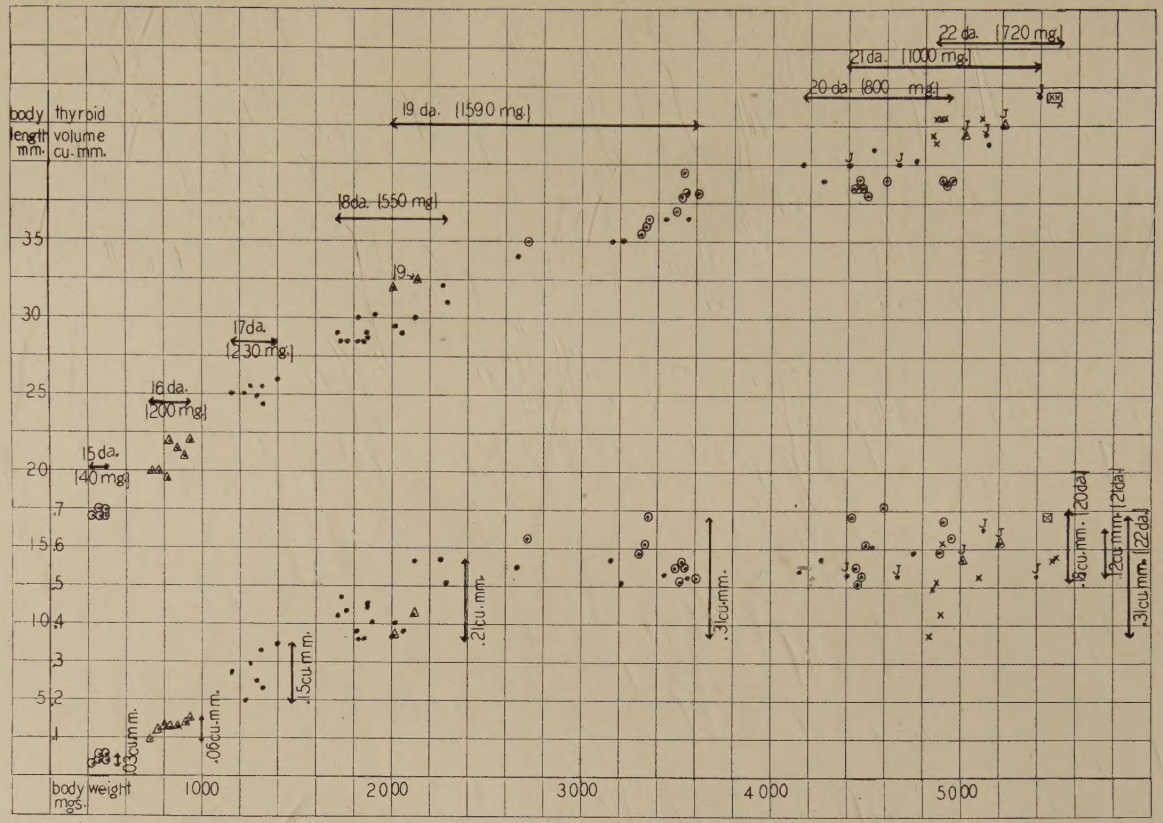

Fig. 1 Variation in weight and thyroid volume of embryo albino rats. Upper curve, body size; lower curve, thyroid volume. Litter mates indicated by enclosing points with symbols △, □ and ○. Since the three ages, 20, 21 and 22 days overlap, the 21-day points are marked by a J and the 22-day points with X. Horizontal arrows — variation in body weight. Vertical arrows — variation in thyroid volume.

given embryonic age and that the individual increases relatively faster in weight than in length. In general, up to 20 days gestation the groups of embryos are distinct from one another in both weight and length. The 20-day embryos, the just-born, and the 1-day-old animals are but slightly longer than the 19-day individuals but show a marked increase in weight. These three older age groups overlap each other. There is considerable variation in thyroid size both within litters at any age and within a heterogeneous group of the same age. This difference between the largest and smallest gland in an age group increases with age, being .06 cu.mm. at 16 days, and .21 to .31 cu.mm. from 19 to 21 days. The thyroid volume calculated per 100 sq.cm. of body surface also shows this variability.

Histological examination of these glands shows a progressive development both of the gland as a whole and of colloid deposition (fig. 2). At 16 days, follicle formation is just beginning with an occasional tiny globule of blue colloid in the lumen. At 17 days, the colloid is evident in many follicles as tiny rounded or triangular deposits. At this stage the colloid

ABBREVIATIONS

bc., blue colloid	sc., storage colloid
cc., colorless colloid	vac., vacuoles in the colloid

Fig. 2 Histological appearance of rat thyroids at the various ages. Unretouched photograps to show amount and distribution of colloid. Magnification, ×300.

A 16 days old. Blue colloid in one follicle.

B 17 days old. Colloid in a number of follicles either blue or colorless.

C 18 days old. Follicles contain either solid blue colloid or blue with colorless droplets. Folliculation almost complete.

D 19 days old. Storage colloid apparent, stained either orange or greenish blue. Folliculation complete.

E 20 days old. Irregular, partially collapsed follicles in the periphery with vacuoles in the colloid, or with a line of colorless colloid at the cell boundaries.

F 21 days old (just born). Irregular, partially collapsed follicles with vacuoles in the colloid near cell boundaries. Majority of follicles with blue colloid.

G 22 days old. Follicles well filled with blue and orange colloid.

H Comparative size and number of colloid masses at 17 and 18 days.

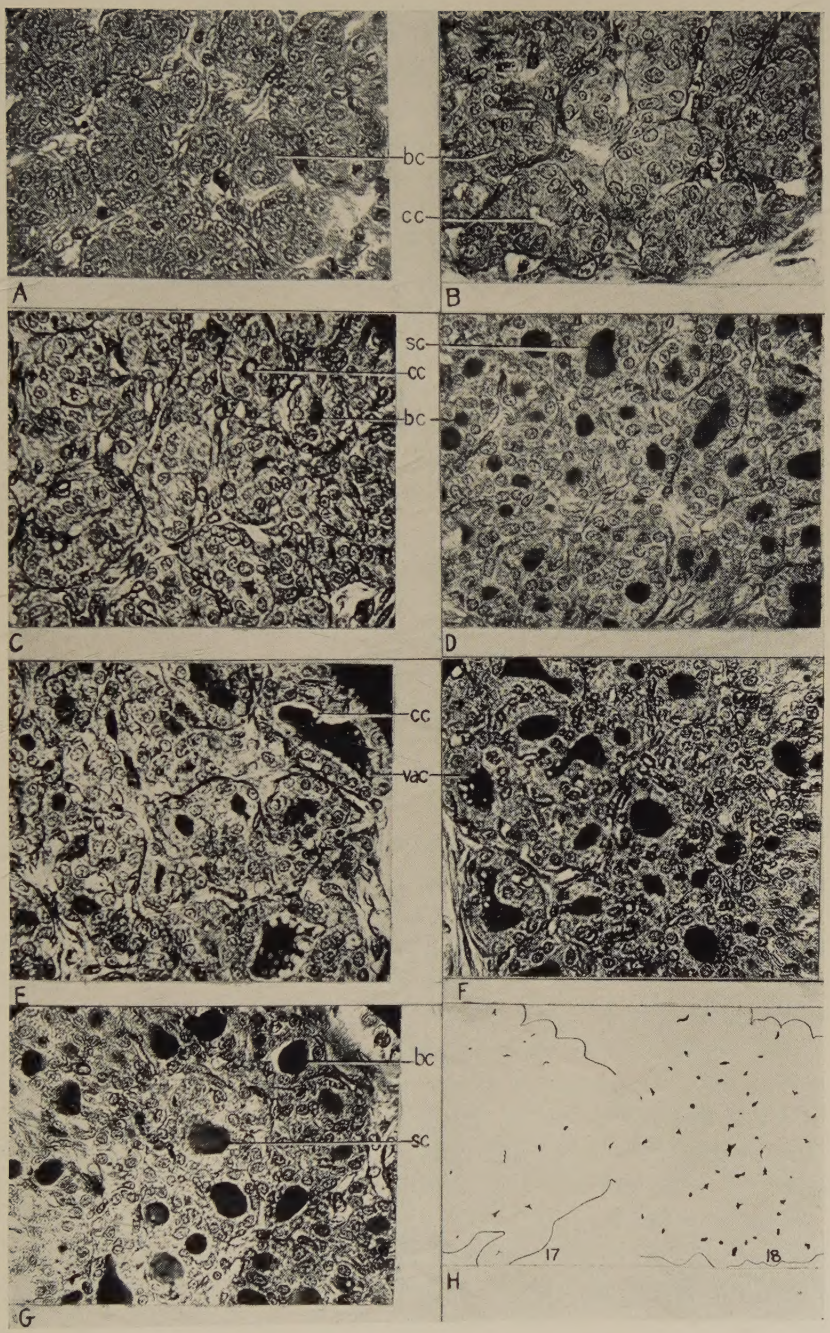

Figure 2

is colorless or stains a deep blue. At 18 days, the follicles have increased in both number and size and are located throughout the gland. At 19 days, large well-filled follicles appear in the periphery of the gland. Most of these follicles take the blue stain but many have a central area tinged with orange or the entire mass may appear greenish. At 20 and 21 days (just born) although there are larger colloid masses containing both blue and orange colloid, many of these are irregular in shape and show large numbers of colorless droplets at the cell margins. After birth, there is a progressive increase of blue colloid accompanied by an increase in size of the follicles. One day after birth, the colloid masses have returned to the well-filled state with the acid storage type again evident.

Kull ('26) reports that the rat thyroid does not become follicular nor show colloid before the nineteenth or twentieth day. Our results are not in accord with this as we found beginnings of colloid formation in follicles at 16 days, and measurable amounts at 17 days. Part of this discrepancy may be dependent on the method of determining the age of the embryos. Kull does not say how he determined the age of his embryos but does report that they were born at 23 days, a longer time than is usual for rats. Long and Evans ('22), using obstetrical cages, found that 90% of all litters were born at 21½ or 22 days after copulation. Allowing for a fertilization time of 24 hours as determined by Huber ('15), we have considered our embryos to be 1 day old at the end of the second day after copulation (the morning of the third day). They were born at 20½ or 21 days of age. If Kull counted the day of copulation as the first day of gestation his 19-day embryo would correspond to our 17-day one. If he counted his animals as 1 day old at the end of the day of copulation then his 19-day corresponds to our 18-day embryo. We then observed colloid either 1 or 2 days earlier than he did.

Kull also compares the rat, pig, and human embryo on the basis of the time at which the thyroid appears and maintains that this occurs relatively late in the gestation period of the rat. At first glance this seems true, but the difference in time

of differentiation in these embryos should be taken into account. In man and the pig, the blastula and gastrula stages are accomplished in a relatively short time. The primitive streak in the pig appears at 13 days or after 10% of the gestation period; in man, it is present at 18.5 days (Jones and Brewer, '41) or after 7% of the total period. The rat reaches this point in development at 9 days or after 43% of the gestation period. Following this, the parts of the body develop in the same relative order as in other forms. The reason for the late development of the thyroid gland, then, seems to be a late start on all differentiation.

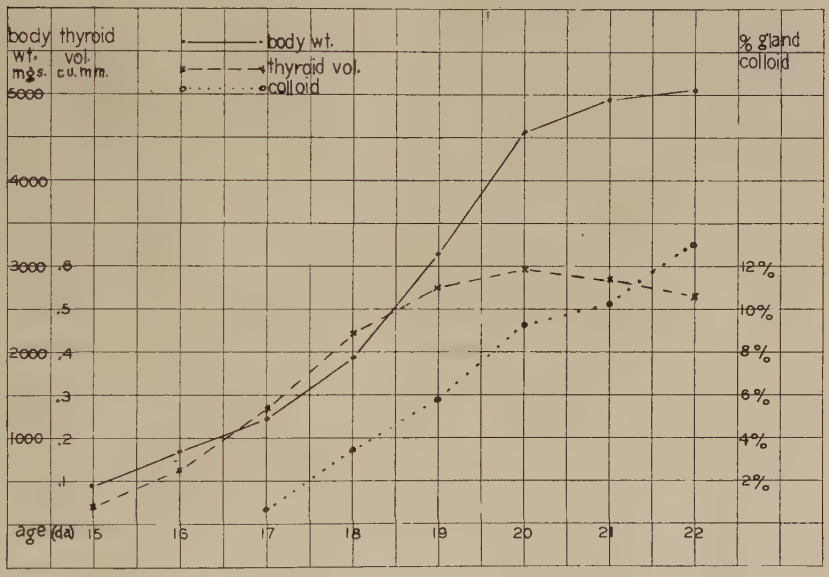

Fig. 3 Increase in body weight, thyroid size, and colloid volume per day.

If we consider that the thyroid is functioning to control the metabolism of the embryo, it is logical to expect its growth to keep pace with the enlarging body. We may ask, then, whether there is correlation between thyroid volume and body weight at the various ages. Calculating the correlation coefficient r, for thyroid volume to body weight we find .096, a very poor correlation. However, considering the colloid as the

significant part of the gland we find that r of colloid volume to body weight is .95 or very good correlation. The correlation of colloid volume to body surface gives the same value, r equals .947, a result which might be expected since surface is a function of weight.

When plotting colloid volume against body weight (fig. 4) the values lie on a straight line for all ages except 20 and 21 days. At these ages the records of individuals lie above

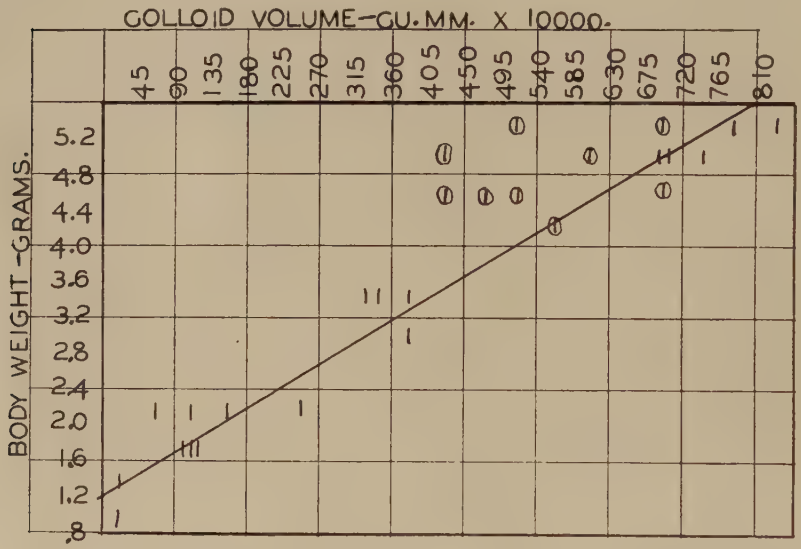

Fig. 4 Correlation of body weight and colloid volume. Circled scores — 20 and 21 days old.

the line, indicating that the colloid volumes are a little small for body size. It appears, then, that there is a constant increase in volume of colloid from the time of its first appearance through 19 days gestation. This evidently represents a progressive differentiation of the gland with the formation of a larger number of follicles or an increase in size of the follicles, rather than an increase in size of the gland as a whole. In fact, the gland ceases to grow in total size at this time (fig. 3). The smaller colloid volume at 20 and 21 days may indicate colloid discharge instead of storage. Further evidence of

this is the resumption of normal relationship on the day after birth, indicating replacement of that which has been used.

The histological evidence corroborates these findings also. At 20 and 21 days the irregular, collapsed follicles with vacuoles at the margins indicate that release of colloid into the circulation is more rapid than storage. Others have described similar conditions after stimulation of the gland by thyrotropic hormone, exposure to cold, and during the combatting of infectious diseases. All these stimuli have been reported to produce the same syndrome in the thyroid gland. The epithelium changes from cuboidal to tall columnar cells, and the colloid decreases in amount leaving the follicle irregular in shape with diverticula. The total volume of the follicle may stay the same or even increase in amount. The cells show globules in the cytoplasm, often in rows from apex to base. These are blue staining. Vacuoles appear in the colloid at the cell boundaries and the mitochondria and Golgi bodies may increase in size. Cramer ('28) and Bailiff ('37) observed these changes after exposure to extreme cold, and Goormaghtigh and Thomas ('34), in connection with various infections. Injection of the anterior pituitary of the frog (Adams et al., '38) and of mammalian pituitary (Okkels, '37; De Robertis, '41; and Williams, '37) gave the same results. Okkels also tested isolated cat and rabbit thyroids in the Lindberg pump. The reaction took a little longer in this case than when the animal was injected with thyrotropic hormone but the results were the same. On the theory that these changes and staining reactions might be artefacts from the chemicals in the fixatives, De Robertis used the freezing-drying method for preservation. The colloid of these glands then stains different shades of blue instead of blue and orange. The dark blue is homogeneous but the light blue colloid shows ice crystals. He believes that the storage type of colloid has less water than the newly-secreted material. Florentin's work ('31) shows the same thing. Others have believed this difference to indicate the presence of more iodine in the colloid of the storage type (Von Hagen) or to be the result of a

combination of chemical reaction and fixatives (Bucher and Bargman, according to De Robertis, '41). Williams ('41) found that, although vacuoles could not be observed normally in the follicles of the living mouse thyroid, they did appear after drying, cooling, or after the injection of various substances. Living follicles in transparent chambers in the rabbit ear (Williams, '37) underwent partial collapse when colloid was released faster than it was produced. Vacuoles were not evident at this point but as recuperation progressed, droplets from the cells were seen to enter the colloid and coalesce with it.

Many workers report that the columnar cells accompany the release of colloid, but Williams describes them during the recuperative stage. We are inclined to believe that columnar cells indicate a high rate of activity regardless of the direction in which the hormone is moving, since from the first appearance of follicles in these embryonic glands the cells are largely columnar.

The depletion effects observed in the 20- and 21-day-old embryos may be a response to the accumulation of pituitary thyrotropic substances in the mother's body just before parturition. Colloid release before birth has been reported for several mammals (Goormaghtigh and Thomas, '34) with the note that if the animal is born in the active condition as is the guinea pig or lamb, refilling of the follicles has occurred at birth but that if born helpless as is the rat or man the refilling occurs after birth. DeQuervain (Cramer, '28) reports this phenomenon in the human and Cramer interprets it as a reaction to cold at birth. It seems more logical to consider it a thyrotropic reaction to the mother's excess pituitary substances since it is present before the exposure to cold.

The physiological activity of these glands as tested by means of tadpole metamorphosis had to be performed over a period of several seasons. In the first season a series of rat embryos was collected for measurements (series 1, table 1), and tadpoles were injected with varying numbers of thyroids taken from embryos ranging in age from 17 to 20 days gestation. These preliminary experiments were planned first, to

find the threshold of thyroid activity, and second, to determine the amount of thyroid substance necessary at the threshold to cause appreciable metamorphic changes. The threshold was determined as 18 days, since ten glands of this age induced 2.5 to 3.0 mm. of leg growth. The 17-day thyroids although used in slightly larger amounts than the 18-day glands did not cause growth of limb buds. Thyroids of embryos older than 18 days caused the same or greater changes with the use of fewer glands.

It then seemed of interest to test the different groups, 18 days and older, to see whether the active material (colloid) was of the same potency at all ages. The fact that in the younger embryos colloid stains blue with Mallory's triple stain, while in later stages both blue and orange staining occurs, raised the question whether these later stages really differed from the younger other than in volume. If the colloid is of the same potency throughout embryonic life, a series of injected tadpoles should all show the same increase in leg length when receiving equal amounts of colloid. If the potency changes with the staining reaction, the tadpoles should differ in their metamorphic changes even though receiving equivalent amounts of colloid.

Taking the colloid of ten thyroids of the 18-day embryos as the standard, the number of glands containing an equivalent amount of colloid was calculated for each of the other ages (table 2). Ten tadpoles were each injected with these amounts

TABLE 2

Calculations of colloid equivalents, taking as the standard dose ten glands of the 18-day embryos.

AGE OF EMBRYO	NO. GLANDS EQUIV. TO STANDARD		CORRECTION FOR 1ST YEAR MEASUREMENTS A/B
	Based on 1 year measurements A	Based on all measurements B	
day			
18	10	10	1
19	5.8	3.75	1.54
20	4.3	2.17	1.98
21	3.4	2.07	1.64
22	2.9	1.74	1.66

for each embryonic stage (series A). Later another series of tadpoles were injected with the same numbers of embryonic glands (series B). At the same time a second series of embryos from the litters used for injections was preserved for measurements. When these calculations of thyroid size and colloid volume were completed it was found that the final averages of all embryos measured were smaller than the figures calculated for the equivalent colloid injections for tadpole series A and B. It was therefore necessary to run a further series of injections based on the final figures (series C). On the supposition that the metamorphic changes in any tadpole were proportional to the amount of colloid injected, a correction factor for each age was determined (table 2) by dividing the number of glands actually injected at each age by the corrected number of glands as calculated from all the individuals measured. When this was done and the resulting factors applied to the tadpoles of series A and B (table 3) it was noted that the amount of leg growth was approximately the same for all the ages within each series whether corrected as in series A and B or whether injected with the proper quantity of colloid as in series C. It is probable, then, that the total volume of colloid injected is the limiting factor rather than the increasing acidity of the colloid as indicated by the orange staining reaction.

We may employ several criteria to sum up our present day knowledge on the time of functioning of the thyroid in mammalian embryos, using as a basis the results of both observation and experiment.

First criterion used — appearance of colloid in the follicles.
Human 60 to 90 days (Kingsbury, '15; Norris, '16).
Pig 50 to 55 days or 70 to 100 mm. (Moody, '10).
Rat 19 days (Kull, '26).
16 days (this study).
Second criterion used — effect of injection of glands on tadpole metamorphosis.
Pig 90 mm. (Rumph and Smith, '26).
Rat 18 days (this study).
Third criterion used — iodine determination on the embryonic glands.
Human 4 months (Lelkes, '33).
Pig 60 days (Rankin, '41).
Fourth criterion used — administration of radio-active iodine.
Rat 18 to 19 days (Gorbman and Evans, '41).

By several criteria, then, thyroid activity is considered to be initiated, in the rat at approximately 18 days of fetal life, in the pig about 52 to 55 days and in the human between 90 and 120 days. In each case evidence of function, at least in a measurable degree, accompanies development of colloid in follicles throughout the entire gland. In the rat embryo there appears to be a gradual steady accumulation and storage of

TABLE 3

Effects of injecting tadpoles with embryo thyroids.

TAD. SERIES	NO. TADS. USED	AGE EMBRYO INJECT.	NO. GLANDS INJECT.[1]	TADPOLE METAMORPHIC CHANGES — AV. GAIN OR LOSS						
				Body loss	Tail loss	Leg gain	Correct factor	Corrected values		
								Body	Tail	Leg
		day								
A	10	18	10	3.9	2.3	3.55	1	3.9	2.3	3.55
	10	19	5.8	3.9	2.3	4.32	1.54	2.5	1.5	2.80
	10	20	4.3	6.0	5.0	5.48	1.98	3.0	2.5	2.76
	9	21	3.4	17.6	13.8	5.5	1.64	10.7	8.4	3.35
	7	22	2.9	6.1	4.3	5.14	1.66	3.6	2.5	3.09
	12	Control	None	2.7	2.6	None		2.7	2.6	None
B	5	19	5.8	4.8	2.4	4.1	1.54	3.1	1.5	2.66
	5	20	4.3	4.1	1.4	5.6	1.98	2.0	.7	2.82
	4	21	3.4	5.5	4.1	4.6	1.64	3.3	2.5	2.80
	5	22	2.9	4.0	1.7	4.3	1.66	2.4	1.0	2.59
	8	Control	None	1.7	.8	None		1.7	.8	None
C	7	18	10	2.2	1.0	2.4	Corrected amounts injected			
	8	19	3.75	2.5	1.6	1.7				
	6	20	2.17	2.4	1.2	2.4				
	6	21	2.07	1.5	.6	2.5				
	10	22	1.74	3.1	2.0	2.4				
	9	Control	None	1.4	.66	.05				

[1] Series A and B — number of embryo glands injected based on first year measurements only.

colloid through the nineteenth day of gestation. Measurements of volume and the histological appearance of the colloid during the twentieth day and at birth indicate a sudden release from the larger follicles, presumably into the blood stream. Nevertheless, in spite of the variation in type of activity of the gland, its potency as marked by the ability to initiate tadpole metamorphosis remains the same.

CONCLUSIONS

1. The thyroid volume has been measured for each day of gestation beginning at 15 days, and the amount relative to body surface determined. There is no correlation between thyroid volume and body size.

2. The amount of colloid at each day of gestation beginning at 17 days has been measured and total volume calculated for each age. There is good correlation between colloid volume and body size.

3. Colloid first appears at 16 days gestation, and is of the so-called active type, staining blue with Mallory's triple stain.

4. At 19 days orange-staining colloid is also present.

5. It has been determined that 18 days marks the threshold of thyroid activity as indicated by a standard reaction of frog tadpoles to the injection of measured quantities of glands.

6. It seems probable that the colloid potency at different ages in the embryo depends on volume rather than on type present (as determined by the staining reaction).

LITERATURE CITED

Adams, A. Elizabeth, Barbara Granger and Ruth Rhoades 1938 Stimulation of the thyroid gland of the guinea pig by Anuran anterior pituitary. Anat. Rec., vol. 72, pp. 491–501.

Bailiff, Ralph N. 1937 Cytological changes in the rat thyroid following exposure to heat and cold, and the relationship to the physiology of secretion. Am. J. Anat., vol. 61, pp. 1–19.

Blandau, Richard J., John L. Boling and W. C. Young 1939 The normal reproductive cycle of the female rat as determined by means of the copulatory response. Anat. Rec., vol. 75, p. 74.

Cramer, W. 1928 Fever, heat regulation, climate and the thyroid adrenal apparatus. Longmans Green and Co., London.

De Robertis, E. 1941 The intracellular colloid of the normal and activated thyroid gland of the rat studied by the freezing drying method. Am. J. Anat., vol. 68, pp. 317–337.

Donaldson, Henry H. 1924 The Rat. Memoirs of The Wistar Institute of Anatomy and Biology No. 6, Philadelphia.

Florentin, P. 1931 Experimental studies and the interpretation of the variations in the color reactions of the colloid in thyroid glands. Compt. rend. Soc. de Biol., vol. 108, pp. 70–72.

GOORMAGHTIGH, N., AND F. THOMAS 1934 Functional reactions of human thyroid; contribution to its histophysiology. Am. J. Path., vol. 10, pp. 713–730.

GORBMAN, AUBREY, AND HERBERT M. EVANS 1941 Time of beginning of function in the thyroid glands of fetal rats. Anat. Rec., vol. 81, p. 95.

HEWER, EVELYN E. 1927 The activity of the thyroid gland in relation to the staining reactions of the colloid. J. Path. and Bact., vol. 30, pp. 621–625.

HUBER, G. C. 1915 Development of the albino rat, Mus norvegicus albinus. J. Morph., vol. 26, pp. 247–358.

JONES, H. O., AND J. I. BREWER 1941 A human embryo in the primitive streak stage (Jones-Brewer Ovum I). Contributions to Embryology, vol. 29, pp. 159–165.

KAAN, HELEN W., AND ADA R. HALL 1937 Anatomical and physiological studies on the thyroid gland of the embryo albino rat. Anat. Rec., vol. 67, p. 64, abstracts.

KINGSBURY, B. F. 1915 The development of the human pharynx. Am. J. Anat., vol. 18, pp. 329–397.

KULL, HARRY A. 1926 The late embryonic development of the thyroid gland of the albino rat. Anat. Rec., vol. 32, pp. 133–141.

LONG, J. A., AND H. M. EVANS 1922 The oestrous cycle in the rat and its associated phenomena. Experimental studies in the physiological anatomy of reproduction. Memoirs of the University of California, vol. 6.

LELKES, Z. 1933 Über den Jodgehalt der Fetalen, Neugeborenen- und Säuglingsschilddrüsen. Endokrinologie, vol. 13, p. 35.

MOODY, R. O. 1910 Some features of the histogenesis of the thyroid gland in the pig. Anat. Rec., vol. 4, pp. 429–452.

NORRIS, E. H. 1916 The morphogenesis of the follicles in the human thyroid gland. Am. J. Anat., vol. 20, pp. 411–448.

OKKELS, HARALD 1937 The culture of whole organs. II. The effects of perfusion on the thyroid epithelium. J. Exp. Med., vol. 66, pp. 297–304.

RANKIN, R. M. 1941 Changes in the content of iodine compounds and in the histological structure of the thyroid gland of the pig during fetal life. Anat. Rec., vol. 80, pp. 123–135.

RUMPH, PAUL, AND PHILIP E. SMITH 1926 The first occurrence of secretory products and of a specific structural differentiation in the thyroid and anterior pituitary during the development of the pig foetus. Anat. Rec., vol. 33, pp. 289–298.

WILLIAMS, ROY GRIFFIN 1937 Microscopic studies of living thyroid follicles implanted in transparent chambers installed in the rabbit's ear. Am. J. Anat., vol. 62, pp. 1–29.

———— 1941 Studies of vacuoles in the colloid of thyroid follicles in living mice. Anat. Rec., vol. 79, pp. 263–270.

THE MECHANICS OF PARAFFIN SECTIONING BY THE MICROTOME

WILFRID TAYLOR DEMPSTER
Department of Anatomy, University of Michigan, Ann Arbor

SEVENTEEN FIGURES

Microtome sectioning involves a type of cutting action akin to that produced by a hand plane, a lathe, or a knife in whittling. Forces are transmitted by the anterior beveled surface of the blade near its edge, and these forces dislodge a superficial layer of the material subjected to the cutting action. This type of cutting may be contrasted with cutting involving more than one surface of the tool -- the chopping and splitting by an ax or the slicing of bread.

An engineering literature (Coker and Chakko, '22; Coker and Filon, '31; Boston, '33; Okoshi and Fukui, '33; and Ernst, '38) has dealt with factors in superficial cutting, but conditions have been so different from those in microtome sectioning that the information may be transferred to only a limited extent. Then too, the primary concern in metal cutting has been directed to surface finish, machinability and the efficient use of power rather than to the mode of chip formation. In microtome sectioning, the chip or section is of major interest.

The primary problem to be considered here is a qualitative analysis of what happens when a microtome knife removes a section of paraffin. Before this may be attacked, however, prior attention must be directed to (1) certain commonly ignored characteristics of the knife edge, and (2) some pertinent properties of the material to be sectioned. Paraffin as the most common embedding matrix will receive primary attention. Though homogeneous masses of paraffin are empha-

sized, the basic conclusions relate also to practical sectioning of tissues embedded in paraffin and to the sectioning of other matrices as well.

THE KNIFE EDGE

Ideal sharpness in a knife may be visualized as the convergence of the beveled facets to a mathematically exact bevel angle. Actually, however, due to the failure of the metal crystals at a knife edge, the bevels do not converge to an exact acute angle. This failure, following Kisser ('27) and von Ardenne ('39), may be defined in terms of the average radius of edge curvature of the actual edge. A small average radius of edge curvature implies relative sharpness or closeness to a mathematically exact bevel. These authors, respectively, have given figures of 0.3 and 0.1 μ as the radius of curvature of a maximally sharp microtome knife. Such measurements are based on edge reflections or on sections through wax or metal impressions of an edge. Since the figures, however, represent measurements at or beyond the limit of resolution of the microscope using visible white light, they lack value as measurements but suggest instead that a convenient standard for edge sharpness is provided by the maximum resolution of the microscope to visible light. Thus, if the edge is examined edge on, it approaches a standard sharpness as edge reflections from a small source of light are reduced to a barely perceptible and even line.

Facet bevels as obtained commercially are arbitrarily standardized and there are apparently no data available as to the best angle for the various types of precision or routine sectioning. A group of knives at this laboratory varied in bevel angle from 19° to 35° with angles near 28° being most common.

Three angles (fig. 1 A) are of significance with the rotary microtome: 1, the bevel angle; 2, the clearance angle, that between the inner knife facet and the plane of the block face; and 3, the rake angle, the angle between a plane perpendicular to the block face and that of the outer honed facet. For a given

knife bevel, the rake and clearance angles are reciprocally related; the sum of the rake angle, the bevel angle and the clearance angle amounts to 90°.

It was shown separately by comparative measurements (Dempster, in press) that sections of homogeneous paraffin without included tissue were less compressed if sectioned with a wide rake angle. As the rake was increased to 72°, the maximum used, distortion became significantly less and this diminished compression was particularly marked for thin sections. Obviously, large rake angles are possible only with thinly beveled knives and with small clearance angles. In the study mentioned, clearance angles as low as 1° were effective if the inner facet was kept clear of gummy accumulations of paraffin. Richards ('42), however, gives evidence that a clearance angle of 4° or more may be of advantage in certain types of actual tissue sectioning.

There is doubtless a limit to the fineness of bevel that may be useful. The average radius of edge curvature is presumably dependent on both the "quality" of steel in a knife and the narrowness of bevel to which a knife is honed. A knife edge was ground and honed from a strip of poor quality steel (band iron) and various bevels, 7° and larger, were prepared. The radius of edge curvature, which was quite large for this material, was greater for narrow than for wide bevels. If edge failure and bevel are similarly related in high quality tool steel, information on the narrowest bevel compatible with specific average radii of curvature would be desirable. Bevels of 16° or 17° to 20° are common in straight razors, razor blades and veneer cutting knives, so it may be presumed that effective edges are possible at bevel angles much below those common in microtomy.

In figure 1, B, a knife edge is shown removing a section; the total forces exerted by the knife in cutting are diagrammed as a series of forces (arrows) normal to the surface of contact between the knife bevel and the paraffin. Opposing forces are also shown. If a knife had an ideal bevel, the micro-forces would have the identical direction along the whole line of

paraffin contact to the very edge. In the actual knife, however, the edge is partly blunted as indicated by its average radius of curvature. Forces here would be directed in a different manner, that is, at a much reduced rake angle, from those characteristic for the beveled facet proper.

If a widely and a narrowly beveled knife of the same average radius of curvature are compared (fig. 1, C), it will be seen that the nominal rake angle is actually interrupted less in the case of the small rake (X′) than where the rake is large (Y′).

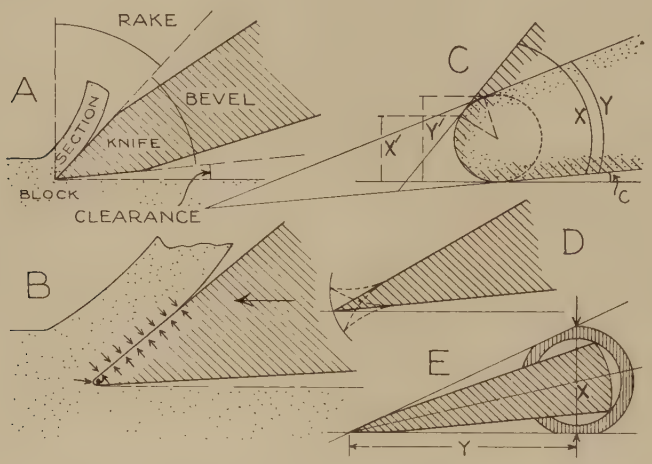

Fig. 1 Aspects of the knife edge. A. Definition of angles associated with knife settings. B. Region of transmission of cutting forces from knife to block and section. Forces, both cutting and resisting forces, are represented as arrows normal to the contact line. C. If X and Y, respectively, indicate a wide and a narrow knife bevel with the same average radius of edge curvature, the interruption of characteristic rake (X′) is less for the widely beveled knife than (Y′) for the narrow bevel. D. Temporary displacements of an edge due to imposed forces. E. When a knife and sharpening back are laid on a flat support, the tangent of the bevel angle is the ratio: $\frac{\text{Measurement X}}{\text{Measurement Y}}$

A further aspect of the knife edge that is augmented by thinness of bevel is edge displacement. For a given knife steel, the amplitude of edge movement due to elastic distortions of the knife edge by imposed forces (fig. 1, D), will be greater for narrowly beveled knives than for stouter types.

Thus, opposed to the demonstrated superiority of narrow bevels in causing less section compression (Dempster, in press) and the theoretical justification of the narrow bevel (von Ardenne, '39), there are limiting factors dependent on edge elasticity and the radius of curvature of the edge (i.e., on the rake differential at the edge and along the outer facet). The problem of possible improvement of these limiting factors is one for the metallurgist.

For most effective sectioning, frictional resistance between a knife bevel and the section being cut should be low. Friction, like a low rake angle, increases compressive strains in the material ahead of a knife bevel. Efficiency implies a low paraffin to steel coefficient of friction and the highest possible facet smoothness.

For each type of sectioning, different types of resistance are met by the knife edge; for precision sectioning, several knives sharpened to different specific bevel angles should be available and should be appropriately selected for specific types of work. Embryonic tissue and other unresistant material, for instance, should be most effectively sectioned with small bevels (i.e., wide rake).

Figure 1, E shows a simple method of determining bevel angle; the ratio of measurements "X" to "Y" represents the tangent of the bevel angle and the angle may be determined and recorded on consulting trigonometric tables. If the edge to back width of a knife is known, the graph of figure 2 will allow the setting of a microtome to a desired clearance angle (cf. sketch and legend of fig. 2) on the basis of one simple measurement. The sum of the clearance and bevel angles if substracted from 90° gives the rake. Through the aid of the graph, a tabulation of various nominal rake and clearance angles may be made in terms of the distance, perpendicular to the block face, between the block face and the mid-point of the heel of the knife.

For intelligent use of the microtome knife, five or possibly six factors should receive attention. These are: bevel angle, sharpness, facet polish, clearance angle, rake angle, and in

the use of the sliding microtome, knife obliquity. The first three factors are determined during honing; the other factors relate to fixing the knife in the microtome.

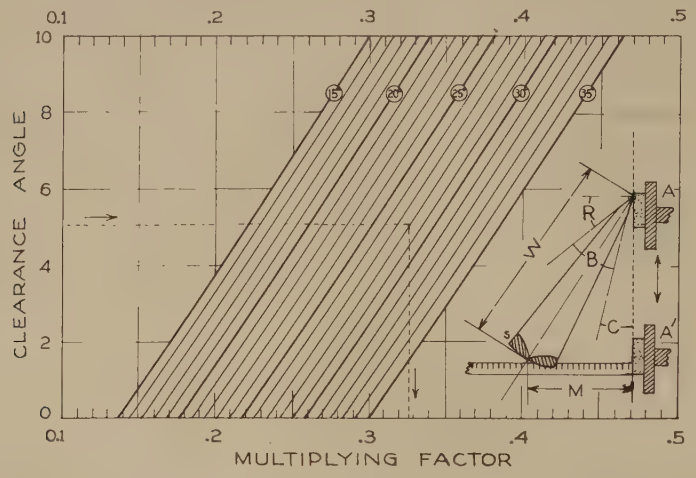

Fig. 2 Chart for determining clearance angle. For a desired clearance angle, e.g., 5°, follow horizontal line to right to intersection with oblique line representing bevel angle of knife at hand, viz., 28°; then follow vertical line to edge of chart, i.e., 0.327. This number multiplied by length W (insert diagram) in millimeters gives the distance M, in millimeters, between the block face and the midpoint of the heel of the knife. Notches in the heel of the knife (s) are helpful. While setting a knife, alternate the position of the block between A and A'.

PERTINENT CHARACTERISTICS OF PARAFFIN

Ordinary paraffin containing no adulterants, if allowed to solidify en masse as in routine embedding procedures, consists of closely packed rod-like crystalline units. Each crystal of the mass has an axial core surrounded by many alternate concentric lamellae of the harder and softer constituents of the paraffin mixture. The size of typical crystals is such — $\pm$ 4 mm. $\times$ $\pm$ 0.1 mm. diam. — that microtome sectioning divides the crystals into a number of slices. Since the characteristic crystalline structure provides a recognizable pattern, an analysis of the distortion and movements that occur in sectioning is possible. This is not as readily accomplished with more homogeneous materials such as celloidin or with other waxy materials.

A microtome section shows a mosaic of crystal slices cut in all planes as would be expected for indifferently oriented crystals. The laminated crystal structure (fig. 3) is clearly shown if a section is momentarily flooded with amyl acetate; this dissolves away the softer paraffin and leaves a skeleton of

Fig. 3 Mosaic of paraffin crystal slices as seen in a 20 μ section of 53-5°C., m.p. paraffin. × 150. Oblique, longitudinal and cross sections show suggestions of lamellar pattern. Black splotches and heavy lines indicate opacity deformation. At the right, flooding of the section with amyl acetate brings out the lamellar structure. Check lines, mostly transverse to direction of cutting (arrow), and stippling suggest disintegrative action of the knife on the lamellar pattern.

harder material. Detailed consideration of the structure and general properties of paraffin is given elsewhere (Dempster, in prep.), and specific attention needs to be directed only to the plastic behavior of paraffin and the mode of reaction to imposed force.

The plastic properties of solid paraffin, which peculiarly characterize the material, change throughout a thermal range. When paraffin is subjected to some specific compressive, tensile, or shearing force at different temperatures, a different type of response occurs above or below some critical temperature that will be called the plastic point. A compression test, adapted from a method of testing dental waxes (Am. Dental Ass'n specification no. 4; Skinner, '40) shows this.

Standard cylinders of paraffin (6 mm. × 10 mm. diam.), cast in a split mould, are compressed over a period of 15 minutes by a standard (2 kg.) weight and the amount of compression of the cylinder is measured at intervals by a dial gauge. Below a critical temperature, compression is slight (fig. 4); above, it is increasingly marked. The specific plastic point and the values of the curve are duplicated only under specified conditions of testing. Shorter or longer application of the standard load gives a different curve; smaller or larger loads also produce different curves, each characterized, however, by a critical transition in paraffin response.

When paraffins of different melting point (m.p.) are tested at one constant temperature, a characteristic compression curve results for each (fig. 5). In general, compression is greater for low melting point paraffin than for paraffins of higher melting point but the two factors are not strictly correlated.

The amount of microtome section compression of different types of paraffin, determined by measurements of section length (Dempster, in press), follows, for equivalent section thicknesses, the order of plastic points. A higher melting point paraffin with a lower plastic point than another sample will compress more. Such behavior can account for the observation of Aumonier ('38) that a 58°C., m.p. paraffin compressed more than a 52°C., m.p. paraffin.

The plastic point, as a temperature above or below which paraffin shows a different mode of behavior to specific strains, becomes a measure of hardness or of relative resistance to

imposed forces and is suggested as a practical measure, better than melting point, for correlating with sectioning behavior. If the type, magnitude and method of application of stress is properly standardized, plastic point should be helpful in distinguishing paraffins.

Compressed cylinders of paraffin are decreased in height and there is a compensatory increase in diameter. Such changes in shape are effected by slipping readjustments of

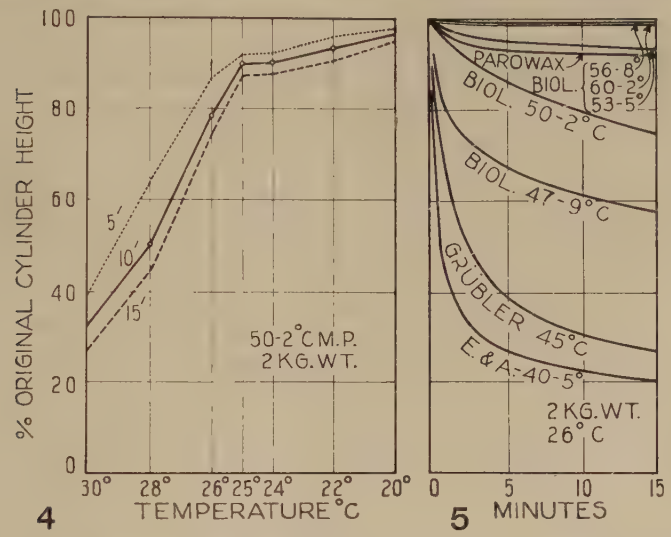

Fig. 4 Curves showing the degree of compression of standard cylinders of paraffin subjected to a continuous load at different temperatures. The amount of compression is shown after application of the weight for 5, 10 and 15 minutes.

Fig. 5 Compression curves representing the shortening of standard cylinders of various melting point paraffins under equivalent conditions. Biol. = Will Corp. Bioloid paraffin; Parowax = from Standard Oil Co.; E & A = Eimer and Amend Co.; melting point ranges indicated by figures.

the relative position of the component crystals. If cylinder height is compressed 12% or more, crystal movements are accompanied by noticeable crystal distortion. With increasing degrees of compression to about 75%, the lamellar pattern of crystals showed increasing disintegration (cf. fig. 3); the main body and particularly the axial region of crystals, however, maintained its essential integrity. With extreme cylinder flat-

tening, all recognizable structure but the axial region of crystals was destroyed.

Since readjustments are effected by slipping movements of crystals in relation to one another and by varying degrees of intracrystalline distortion as well, one obviously must consider the resisting forces, that oppose deformation and prevent complete collapse of the material under stress, as operating both at crystal boundaries and within the substance of crystals. Thus, the resistance of cylinders to complete flattening under a compressing load is in reality the sum of the inter- and intra-crystalline resistances to shearing movements. Such resisting forces are cohesive in character and are relatively greater below a critical transition temperature than above.

The significant variables relating to paraffin plasticity, as indicated in figures 4 and 5, are: load, time of action of the stress, temperature, and resistance to distortion.

When paraffin is compressed suddenly by a large load — a hammer blow or compression between vice jaws — it becomes bruised and shows a whitish opacity unless the temperature is within about 20° of the melting point. Opacity becomes marked at colder temperatures, and after cooling paraffin in ice water, it pulverizes or shows gross fractures. Opacity is due to minute cleavages and air spaces occurring both at intercrystalline junctions and at the peripheral (chiefly) lamellae of crystals.

Cleavages in stressed cold paraffin decrease the density of the paraffin materially. Volume measurements by water displacement (water containing the surface active agent terpitol), when made on 50-2°C., m.p. paraffin rendered opaque at room temperature by a hammer blow, showed a 4% volume increment. Greater increments (15–16%) were found when paraffin at room temperature or in ice water was shaved by a scalpel into fragments about $\frac{1}{2}$ mm. thick. Opacity and decreased density did not appear or were negligible for similar shearing at a temperature of 38°C.

THE NATURE OF THE CUTTING REACTION

Photoelastic studies by Coker and Chakko ('22), Coker and Filon ('31) and Okoshi and Fukui ('33), though made to interpret aspects of metal cutting, provide some information on the nature and direction of forces active in all types of surface cutting. Stresses during cutting were computed and figured in stress diagrams like figure 6 A and B.

The major forces exerted in cutting are differentially distributed through both the tool and the material being cut. As the radial distance from the line of tool-material contact,

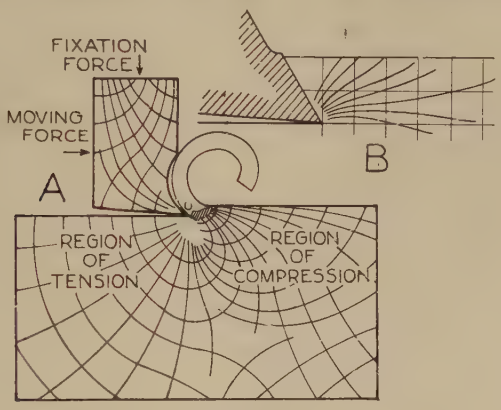

Fig. 6 A. Stress diagram of milling machine tool cutting a chip (modified from Coker and Filon). The shaded area near O indicates the region of plastic deformation. B. Lines of principal shear in the region ahead of a knife edge (from Okoshi and Fukui).

"O," is increased, the stresses (force per unit area) are dispersed over a larger and larger area. Conversely, in the region near "O" (shaded area), stresses acquire such magnitude that the elastic limit of the material being cut is exceeded. Permanent deformation or fracturing occurs here. It will be noted that the region of deformation is both below and above the level of the knife edge. Though the photoelastic method does not indicate the nature of the disturbance in a plastically deformed region, the stress pattern in neighboring regions is pertinent. Material ahead of the knife bevel is subjected

to horizontal compressive stress. Behind the knife edge, in the region of the new surface, the material exhibits horizontal tensile stress. Material at and below the knife edge is lifted in a vertical direction by tensile forces. The resultant of forces ahead of the knife bevel may be shown as lines of principal shear as in figure 6, B. Movements of material due to sectioning may be expected to follow such shear lines.

Behavior in the plastically deformed region ahead of a knife bevel may be inferred from a study of rather thick (2–3 mm.) sections of paraffin. To produce such sections, a block of paraffin at some temperature 20° or more below the melting point, is simply placed between vice jaws with 2 or 3 mm. of the edge projecting above the jaws, and a knife or chisel edge, straddling the jaws of the vice, is shoved along at a constant velocity to detach a section.

As shown in figure 7, sections acquire a segmental character as they form and curl at the knife edge. They consist of tranverse prisms of clear paraffin between which are thin regions (stipple and lines) of opaque paraffin. When sections are cut with a wide rake knife, the segments of clear paraffin extend through the whole thickness of sections. Their profile in the axis of knife movement (fig. 7 A and B) is approximately rhomboidal. The laminae of opaque paraffin between the prisms are thin and even, except at their lower extremities where they become wider. Each prism slightly overrides the next in sequence so that a perceptible serration is evident on the free surface. Prisms, thus, shear and slip along lines of opaque paraffin. As the knife tilt is increased (fig. 7 C and D), the opaque paraffin increases and slip planes appear to have encroached on the basal region of the clear prisms. These latter now have rounded basal regions and ordinarily do not extend through the whole thickness of the sections. As the knife rake is further decreased, the overriding of prisms along oblique 45° planes results in more marked imbrication on the free surface. At a rake of 30°, as much of the corrugated outer surface is made of exposed slip plane as of the original paraffin surface. With a still further decrease in rake, the

prisms of clear paraffin now have a roughly triangular cross section. As the knife rake is decreased to zero or beyond (fig. 7 F and G), the opaque interprismatic paraffin is crushed and formed into a narrow strip which becomes moulded into the lower edge of each triangular prism.

Clear prisms, particularly those made with narrow rake knives are themselves deformed by cutting. When a section is flattened (fig. 7 J), the segments separate partly and it becomes obvious that they could not be reassembled to form a

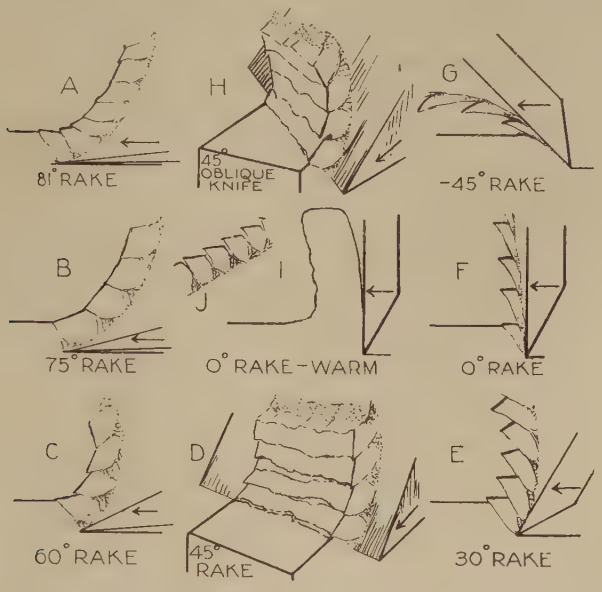

Fig. 7 Structure of thick paraffin sections for various knife rakes. Stipple and fine lines indicate regions of paraffin opacity. Arrows show direction of knife or chisel movement. At "J", a section, 45° rake angle, is shown uncurled and flattened.

continuous layer of paraffin without remoulding the shape of the prisms. Thus, sectioning involves, in addition to gross shearing movements over lines of opacity, minor shearing and moulding movements that do not involve opacity and ruptures. This moulding action increases as rake angles become narrower.

As a segment of a section lifts upward to move across the face of a knife bevel, its direction is changed, and from a series of such segments a curled section forms. The inner side of the curl is compressed and the serrations at the surface are compensatory; the outer side is under tension. The forward movement of the knife and frictional forces as well, compact and crush, and for narrow rakes remould, this basal region of sections; in all cases, the basal surface of sections becomes burnished and shiny.

If the block from which sections have been removed is examined, one sees slight transverse grooves marring the surface. The more prominent are as far apart as the width, across the upper surface, of the clear prisms making up the section removed. Between these major grooves are four or five others which may be barely perceptible. Obviously, these markings are due to downward deflection of the knife edge during moments of slip plane formation. The major grooves are associated with the breaking off of clear prisms of paraffin and the minor with the secondary slip planes that appear in the basal regions of sections. When a knife edge is deflected downward by paraffin resistance, it acquires increasing amounts of energy which are suddenly released when the elastic limit of the overlying paraffin is exceeded. The springiness of the knife edge, in effect, pries up the paraffin and a slip plane is produced together with a shear movement of the newly formed prism of paraffin. Knife elasticity thus imparts an oscillatory rhythm to the forces active at a knife edge during cutting.

Ernst ('38) has illustrated exposures from a motion picture film of a narrow rake knife impinging on a block of paraffin in the first act of removing a section. At the point of impact as seen from the side, the paraffin is deformed and shows as a tiny opaque triangle extending above and below the knife edge with an apex directed forward in the axis of knife movement. The opaque triangle increases in size and the apex further invades the clear paraffin till finally a slip line or fracture, beginning at the apex of the triangular area, extends

forward and upward to meet the surface of the paraffin being sectioned at an angle of about 45°. Thus, the first prism of paraffin is displaced, but the knife has scarcely entered the paraffin. Now, as shown in figure 7, the knife edge moves forward into the region from which the prism was broken. New slip planes of a minor type, often four to six of them in succession, form and course upward to meet the slanting surface of the first major slip plane, again at an angle of about 45°. By the time these reach a length of about half the section thickness, a long arching major slip line breaks through to the surface, and a second clear prism is removed. As the knife moves along, shearing several minor prisms and then a major one in alternation, forces are causing prism slippage, basal crushing, moulding, readjustments within prisms, and the burnishing of the basal surface of the section as indicated above.

Sections made above some critical temperature involve an entirely different type of cutting reaction. In warm sectioning, the sections are continuous, are relatively translucent and are shorter than equivalent sections made with colder paraffin (fig. 7 I). The type of cutting and the displacements of material by the knife edge are, in general, similar to those found in the continuous chip type of cutting of ductile metals (Ernst, '38). Built-up edges that may occur on the outer bevel of a tool in the cutting of ductile metals, however, do not occur with paraffin. The knife moves smoothly across the block and the paraffin responds by smooth shearing flow movements extending obliquely from the knife edge to some point on the surface a short distance ahead of the knife edge. This oblique plane of shearing, which limits the anterior end of a section as it forms, lies at about 45° to the block surface and this seems to be true for all rakes. Along this plane, sliding and squeezing movements of crystals occur and the lamellar pattern of crystals is disturbed. Shear lines may traverse certain crystals. Transversely placed crystals ahead of a knife edge, as seen from the side, though not yet severed, are bowed and internally deformed. In thinner sections, ap-

proaching a crystal diameter or less in thickness, crystal boundaries may become indistinct and the lamellar pattern becomes distorted. Distortion is effected by plastic flowing movements of the material of both crystals and intercrystalline junctions. When block temperature is lowered below the plastic point, opacity and discontinuous shear movements suddenly begin.

The energy involved in shear movements and the frictional forces between a knife and a section liberate heat. In a poor conductor such as paraffin a slight local increase in temperature could have only a localized effect in altering the plastic behavior of paraffin. In thin sections, even though the block and working temperature are relatively low, the thermal effect on plasticity, due to sectioning, is distributed over a larger proportion of the section thickness than for thick sections. Accordingly, the mode of sectioning follows the plastic flow (warm) type of cutting even at moderately low room temperatures. As sections are made thinner and thinner, the local warming effect increases materially. Crystal distortion becomes extreme and gross shortening of sections becomes marked. Some correction of this defect may be made by lowering block and particularly the knife temperature so that excess heat is absorbed. The local thermal effect is less also with paraffins of high plastic point.

In addition to warming effects that are particularly marked for thin sections, a local lowering of the temperature of transition may be expected due to the increased stress associated with thin sections. Bridgeman ('16) has shown that a solid subjected to any stress experiences a depression of the temperature of transition between two phases. If the stress differential is great enough, plastic flow is produced by actual local melting followed by regellation and the equalization of pressures in the component particles of the material subjected to strain.

A type of sectioning response that is most desirable in microtomy is a transition between warm and cold sectioning. It occurs only for rakes beyond about 50° and for intermedi-

ate thicknesses of sections (roughly 10 to 200 microns or more) when sections are made at temperatures just below the transition point. Narrower rakes and a marked decrease in temperature cause prismatic sections. Prism size is proportional to section thickness. The intermediate type of section has a velvety upper surface and a somewhat generalized opacity. Magnification shows this opacity and diffuse shearing effect to be located primarily at intercrystalline boundaries though minor opacities may appear within crystal outlines. The crystal slices are commonly tilted obliquely.

This type of sectioning, characteristic of wide rake angles and a suitable balance between paraffin plastic point and cutting temperature, produces less displacement of crystals, less deformation and less shortening of sections grossly than the typical warm or cold types of sectioning. Such sections, of course, adhere well to form ribbons with the rotary microtome. Shortening of sections amounts to 20% or less of block length. This diffuse intercrystalline type of shearing may be extended to the thinner range of sections somewhat by the reduction of local warming effects as indicated above.

ASPECTS OF MICROTOME SECTIONING

Various aspects of routine sectioning may be illustrated by placing an elongate block of paraffin in the microtome, drawing a knife, set at a right angle to the axis of movement, almost across the length of the block and then withdrawing the knife. The block with the attached section is then removed and carefully laid on its side in an embedding box. A low melting point wax, having a distinctive crystal structure (diglycol stearate + soft paraffin; 50:50) and preferably colored, is poured over the block and section. On cooling, microtome sections of about 25 microns thickness, are cut across the side of the block. Such sections of sections as illustrated in figures 8 to 12 represent sectioning at one room temperature.

Figure 8 shows the result of plastic flow in a 10-micron section. Slip lines, extending from the knife edge, proceed through the whole thickness of the section to meet the block

surface at about 45°. Figure 9 shows a thicker section cut from the same block with evidence of intercrystalline slippage (at a) and plastic flow (at b). Such intercrystalline vacuities as that illustrated at "a," form the basis for opacity. In figure 10, the split below the crystal at the knife edge is further

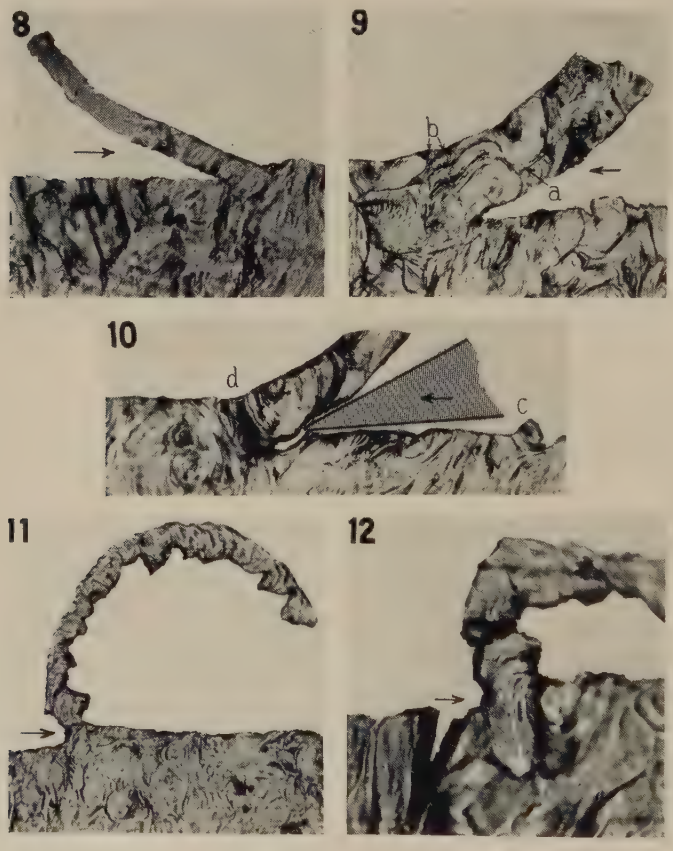

Fig. 8 Longitudinal section through a 10-micron paraffin section and block showing distortion due to sectioning. × 175. This and the accompanying sections were made with a transverse knife at a rake of 60°; 56-8°C. m.p. Bioloid paraffin; 27°C. cutting temp.

Fig. 9 One hundred-micron section seen in longitudinal section. × 100. Distortions indicated by letters are discussed in text.

Fig. 10 Fifty-micron section. × 100.

Fig. 11 Fifty-micron section made with a dull knife. × 50.

Fig. 12 Thirty-micron section made with a dull knife. × 175.

evidence of intercrystalline movement — movement, however, in this case, associated with rupture at a crystal boundary. This is shown, likewise, by the crystal to the right at "c". Planes of plastic slip are evident at "d". The protruding ends of crystals left at the block surface suggest a breaking of crystals, one by one, by slip planes acting reasonably close to the plane of knife edge movement.

Figures 11 and 12 illustrate the effect of cutting with a very dull knife edge. Planes of slip similar to those shown above in figure 7 for thick sections cut with a knife rake of 0° to 30° are clearly evident even though the nominal knife rake was the same as that used for the other sections, and cutting was done in an identical room temperature. These figures indicate that a dull knife has the same effect as a strong reduction in rake of a sharp knife. Conversely, it may be assumed that the effect of a sharp knife in microtomy is to allow a constant rake to exert simple, unmodified shearing forces to the very edge of the knife.

Figure 12 is remarkable, in addition, for showing a knife edge impinging on a crystal in such a way as to suggest the mode of action of cutting forces (cf. photoelastic method, p. 251). The region ahead of the split appears to be horizontally compressed, that behind is tensed. There is an obvious lifting and prying effect (vertical tension) on the crystal ahead of the knife edge. Intracrystalline shear lines are suggested.

When sections showing various degrees of shortening are viewed normally, the amount of paraffin crystal distortion is seen to be proportional to the degree of compression in section length. Figures 13 to 16 show the change in crystal pattern for four different section thicknesses. In thicker sections, small interstitial crystals and crystals lying parallel to the knife edge are compressed most, while crystal cross sections maintain their shape and structure. With the greater distortion of thinner sections, crystal cross sections appear compressed and the peripheral regions break down. Meanwhile, longitudinal crystals are further distorted. In very thin sec-

tions, all evidence of crystalline structure disappears except crystalline cores and a few adjacent lamellae (fig. 16). Crystal distortion in sections is thus very much like the distortion found with cylinders of paraffin subjected to compressing loads.

Intercrystalline junctions give way and crystal slices come to occupy oblique planes in the section. This is shown in the dark transverse crystals of figure 14, in which the loss of brightness is due to the refraction of light away from the lens of the microscope. Crystal edges last to pass over the knife

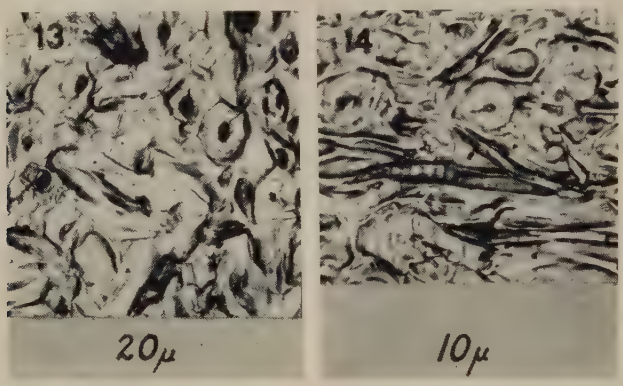

Fig. 13 Structure of a slightly compressed paraffin section (to 83%) showing crystal cross sections with prominent axial regions and hexagonal boundaries. The lower gray area indicates the amount of section shortening as compared to original block size. 50-2°C. m.p. paraffin; 24°C. cutting temp.; × 100.

Fig. 14 A more compressed section (to 75%).

edge are raised to produce a shingle-like surface. This imbrication becomes pronounced with small knife rakes or with moderately great compression.

Intracrystalline plastic readjustments which occur within crystal slices are illustrated best in cold sectioning. One part of the crystal slides against another along slip planes. Usually groups of parallel slip planes (fig. 17) are found. Ordinarily, they form transversely to the axis of knife movement and are particularly prominent in crystals with long axes in the axis of knife movement. Slip planes also may follow the lamellae of the crystal pattern. The surface overlying groups of slip

lines, as shown by oblique reflected illumination, is thrown into parallel ridges like the surface of a file. Such distortions may be accounted for by intracrystalline plastic shearing movements of a type extensively studied in relation to plastic flow in metals (Bingham, '22; Nádai, '31; Rosenhain and Haughton, '35; Houwink, '37; Crane, '39; and Andrade et al., '40).

With warm sectioning and with the cold sectioning of thin sections, such intracrystalline shear lines are not clearly evident. Instead, the pattern of crystal slices, and the intercrystalline junctions as well, is broken up by plastic or viscous flow movements of a submicroscopic character.

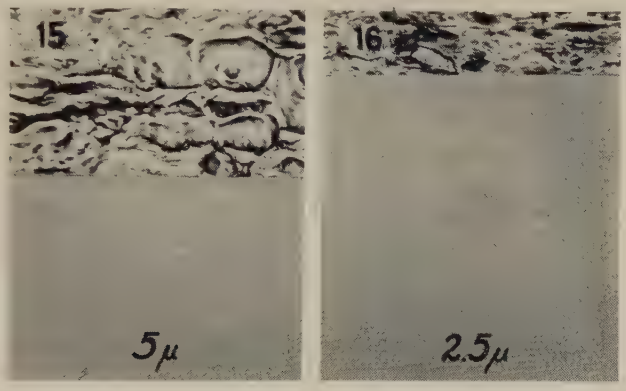

Fig. 15 A section compressed to 45% of block length. Crystal cross sections are still recognizable. Transversely, across the middle of the section is a junction between two sections in a ribbon. Distortion is more marked for the end of the first section (lower) than for the beginning of the second.

Fig. 16 An extremely compressed section, to 18%, showing loss of all structure except for three or four crystal cores and adjacent lamellae.

Plastic shear lines and crystal imbrication give an uneven surface to sections and the surface appears velvety to the naked eye. Discontinuities, chiefly at intercrystalline boundaries, by their opacity contribute also to the velvety appearance; sections made at a sufficiently higher temperature are more translucent.

Both shear movements and the obliquity of crystal slices cause sections to be much thicker than the microtome setting. Decreased section length is in reality a compensation.

Richards ('42) finds that section thickness is actually more than enough to compensate for section length if section volume is based on block area and microtome setting. This "excess thickness" is no doubt accounted for by opacity and the resulting decreased density.

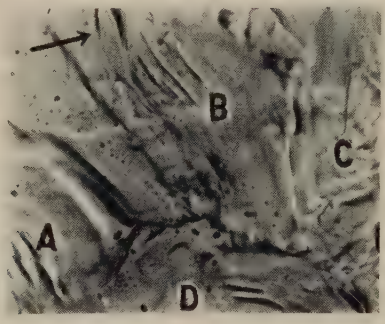

Fig. 17 Parts of four crystals of paraffin (A, B, C, D), each showing groups of intracrystalline slip lines. Arrow indicates direction of knife movement. × 450.

SECTIONING OF TISSUES

Observations on a wide variety of animal tissues, infiltrated and embedded in paraffin, show that tissues participate in the cutting reaction in a manner quite the same as paraffin. In the cold cutting of intermediate and thick sections, the tissue is divided into segments; the shape of segments for specific rakes is like that for paraffin; the basal region of sections is similarly crushed. In warm sectioning, point by point shearing occurs. Like paraffin, thin sections of tissue show the effect of local warming by frictional heat and the distortions are more marked for the thinner sections. Under the special conditions for diffuse discontinuous shearing at temperatures near the plastic point there are some appearances that suggest similar action.

Differences between tissue and paraffin sectioning are largely differences in degree of response. Tissue embedded in paraffin provides a mesh, the constituent parts and interstices of which are permeated with paraffin. The material of

the mesh is a gel and the pertinent properties of this gel — renitency, hardness, brittleness — are dependent on the original nature of the tissue elements during life and the colloidal and chemical alterations due to fixation, dehydration, clearing and infiltration. Shrinkage and heat effects likewise may affect such properties. Thus, the physical characteristics of a tissue mesh are assuredly different from paraffin and one tissue (or fixation sequence) differs from another. The component resistances to cutting of a meshwork and its interstices may be expected to differ from the general matrix of paraffin.

In general, cleavages in the tissue meshwork do not occur as readily as in paraffin, unless the tissue is brittle, the rake angle small or the cutting temperature too far below the plastic point. Brittle tissue — yolk filled regions, colloid, etc. — may segment while the paraffin matrix adjusts by smooth plastic flow movements. Cartilage or a celloidin matrix infiltrated with paraffin, on the other hand, may show plastic flow movements while the matrix paraffin is sheared into segments. Masses of connective tissue may respond to cutting forces by fibrous tearing with a resultant opaque and disturbed block surface. The next section then is made through inadequately supported tissue. Due to the variable resistances of tissues, the amount of section shortening may be slight or extensive; tissue compression is rarely as extensive as the compression of sections of the embedding paraffin alone (Dempster, in press). Embryo tissue, however, offers so little resistance to sectioning that sections shorten about as much as for paraffin alone; corrugations in sections after floating, thus, are uncommon.

Obviously, effective sectioning calls for approximately the same elastic and plastic properties in both tissue and matrix. Avoidance of undue hardening by fixation and other procedures, the procedure of infiltrating in a low plastic point paraffin and embedding in a harder one and the appropriate adjustment of cutting temperature may be necessary prerequisites for suitable sections. Celloidin double embedding

methods tend to induce, in otherwise brittle tissue, smooth plastic adjustments like those characteristic of celloidin alone.

The sectioning process characteristically imparts a curl to sections; the particles of both tissue and matrix are deformed in congruence with the curling distortion. If sections are thin or if sections are warmed or floated on water, they flatten, but the flattening process does not involve the same type of plastic change as that causing the curl, and transverse fractures may now occur. Thyroid colloid and intravascular clots, as seen in microscopical sections, often show this defect. It is illustrated also if hard wood shavings from a plane are uncurled and flattened.

Examination of microscopical sections with a view to recognizing and evaluating deformations due to sectioning is made easier if poor slices — brittle material, defective ribboning, scoring by a nicked knife — are selected. Minor deformations of sectioning, though present, are difficult to distinguish because superimposed on the sectioning defects are changes due to colloidal swelling adjustments occurring in flattening procedures and the staining sequence. These mask and in part compensate for the lesser sectioning defects (Dempster, in press).

SUMMARY AND CONCLUSIONS

The microtome knife is a surface acting cutting tool that removes a section by causing shearing movements in the material being cut. Two primary types of shearing response are characteristic in the sectioning of paraffin or of paraffin infiltrated tissues and the type of response depends on the working temperature. Cold sectioning, which is characterized by discontinuous shear movements of material, occurs below a particular critical temperature for each type of paraffin and warm sectioning, sectioning in which shear movements occur continuously in point to point sequence, appears above this temperature. With a relatively flat knife tilt and for intermediate thicknesses of sections, cold sectioning is effected by diffuse shear movements occurring primarily at the inter-

crystalline boundaries of the paraffin matrix. For these special conditions, minimum total distortion is obtained. In the case of thinner sections, heat dissipation in the region of shearing elevates the temperature locally, and sectioning follows the warm type of reaction. Sections show considerable compression. Through the selection of suitably hard embedding matrices and by drawing off frictional heat (with a cold knife), it may be possible to reduce compression and transform the cutting response of thin sections from the warm to the intermediate diffuse shear type.

Paraffins of different hardness show varying degrees of resistance to shearing. Hardness may be determined through paraffin plastic points, that is, by the critical temperature above or below which paraffin responds in a different manner to some specified stress. Celloidin does not show a thermal response for thin sections like paraffin does; though the material is relatively resistant to distortion, it presumably sections by point to point plastic flow like warm paraffin.

Material embedded in paraffin may be considered as a gel in which the aqueous phase has been largely replaced by paraffin. It acts as a resilient web following the movements of the paraffin matrix but increasing the resistance to shearing flow. Section compression is less than for the matrix and this effect is more marked for dense tissues, such as cartilage or heart muscle, than for looser tissues, like embryonic material or lung. When tissue is rendered brittle by fixation and related procedures or contains inclusions that are not readily penetrated by paraffin, fracture lines and crumbling may result.

For a given material and matrix to be sectioned, the desirable aspects of a knife, as inferred from the foregoing, are:

1. As narrow a bevel as is consistent with a low average radius of edge curvature and a low amplitude of edge deflection under the resistances met in sectioning.
2. A low average radius of edge curvature. This is particularly important for thin sections. Knife acuity and a narrow bevel allow a wide rake angle to be effective over nearly the whole

line of contact between the outer bevel and the material being cut.

3. A low resistance to the sliding of a section across the outer bevel. This implies bevel polish, freedom from scratches of appreciable size and as low a coefficient of friction with the material being cut as is consistent with the other properties of the knife.
4. For thin sections, a cool enough knife edge to carry away frictional heat losses.

The first three characteristics have in common a reduction in the magnitude of an anteriorly directed compressive force on the material ahead of the knife bevel. If compressive forces are augmented by a blunt edge or a rough bevel surface, the effect is similar to a decrease in rake angle. A decrease in temperature, by altering paraffin resistance, has an indirect effect in increasing the magnitude of edge deflection. An increase in load, due to increased section thickness, has a similar effect. Temperature changes also alter the adhesiveness of paraffin to a knife bevel. The effectiveness of the water-on-the-knife method of sectioning with the sliding microtome is probably as much due to the prevention of adhesion of sections to a knife as to surface tension effects.

LITERATURE CITED

ANDRADE, N. DA C. ET AL. 1940 Report of a conference on internal strains in solids held at the H. H. Wills Physical Laboratory, University of Bristol. Proc. Physical Soc., vol. 52, pt. 1, pp. 1–178.

VON ARDENNE, M. 1939 Die Keilschnittmethode, ein Weg zur Herstellung vom Mikrotomschnitten mit weniger als 10^{-3} mm. Stärke für elektronen mikroskopische Zwecke. Zeit. f. wiss. Mikroskopie, Bd. 56, S. 8–23.

AUMONIER, E. J. 1938 Notes on the distortion of paraffin sections. J. Roy. Micr. Soc., Ser. 3, vol. 58, pp. 253–257.

BINGHAM, E. C. 1922 Fluidity and plasticity, pp. 440, McGraw-Hill Book Co., N. Y.

BRIDGEMAN, P. W. 1916 On the effect of general mechanical stress on the temperature of transition of two phases, with a discussion of plasticity. Phys. Rev. (Ser. 2), vol. 7, pp. 215–224.

BOSTON, O. W. 1933 Engineering and shop practice, vol. 1, pp. 539, John Wiley and Sons, N. Y.

COKER, E. G., AND K. C. CHAKKO 1922 An account of some experiments on the action of cutting tools. Proc. Inst. Mech. Engineers, vol. 1, pp. 567–621.

COKER, E. G., AND L. N. G. FILON 1931 A textbook on photoelasticity, pp. 720, Cambridge University Press.

CRANE, E. V. 1939 Plastic working of metals and power press operations, pp. 450, John Wiley and Sons, N. Y.

DEMPSTER, W. T. Paraffin compression due to the rotary microtome, Stain Tech., vol. 18. (In press.)

——— (in prep.) Properties of paraffin relating to microtechnique.

ERNST, HANS 1938 Physics of metal cutting, pp. 1–34. Machining of metals, pp. 177, Am. Soc. for Metals, Cleveland, O.

HOUWINK, R. 1937 Elasticity, plasticity and the structure of matter, pp. 376, Cambridge Univ. Press, Cambridge.

KISSER, J. 1927 Methoden zur Bestimmung der Winkelgrössen an Mikrotommessern. Zeit. f. wiss. Mikroskopie, Bd. 44, S. 452–459.

NÁDAI, A. 1931 Plasticity, a mechanics of the plastic state of matter, pp. 349, McGraw-Hill Book Co., N. Y.

OKOSHI, M., AND S. FUKUI 1933 Researches on the cutting action of planing tool, by mikrokinematographic, photoelastic and piezoelectric methods. Sci. Papers Inst. Phys. and Chem. Rps. (Tokyo), vol. 22, pp. 97–166.

RICHARDS, O. W. 1942 The effective use and care of the microtome. Spencer Lens Co., Buffalo, N. Y. (In press).

ROSENHAIN, W., AND J. L. HAUGHTON 1935 An introduction to the study of physical metallurgy, pp. 368, Constable and Co., London.

SKINNER, E. W. 1940 The science of dental materials, pp. 421, W. B. Saunders, Philadelphia.

DISTORTIONS DUE TO THE SLIDING MICROTOME

WILFRID TAYLOR DEMPSTER
Department of Anatomy, University of Michigan, Ann Arbor

ONE FIGURE

The foregoing paper on the mechanics of sectioning and a study of the extent and characteristics of section distortion by the rotary microtome (Dempster, '42; '43, in press) have dealt in some detail with the distorting effects of the sectioning reaction for the transverse knife. Extension of the analysis to certain reactions in oblique cutting by the sliding microtome reveal general relationships that pertain to both the sliding and the rotary microtome.

The rotary microtome has a knife axis set at 90° to the axis of block movement, whereas in the sliding microtome, the knife is ordinarily fixed obliquely to the axis of movement. When a knife is set obliquely, a greater length of knife edge and a greater effective area of the outer facet of a knife are employed in sectioning.

An imaginary plane, simultaneously parallel to the axis of knife movement and perpendicular to the block face of the material being sectioned, may be visualized as intersecting the outer bevel of a knife in the sliding microtome. If the knife is at a right angle to the axis of movement, i.e., comparable to the position in the rotary microtome, the imaginary plane intersects the outer bevel at a smaller rake angle [1] than if the knife were set obliquely. Similarly, if the obliquity of a knife is changed from a transverse position to a position where its edge coincides with the axis of knife movement, the

[1] The rake angle or normal rake of a knife is the angle, in a plane transverse to a knife edge, between the outer beveled facet and the perpendicular to the new block surface.

rake angle in the axis of knife movement increases to a maximum of 90°. A knife with an obliquity of 45° has the same rake angle directed to the side as it does anteriorly. As the knife set is made more nearly transverse to the axis of movement, the side rake increases and the anterior or front rake decreases toward a minimum value; conversely, side rake decreases and front rake increases as the knife obliquity approaches the axis of movement. Some effect may be postulated as due to this unsymmetrical relationship of front and side rakes.

If a 90° knife passes almost across the face of an elongate block of paraffin in the cutting of a section, the knife may be backed away in order to leave the partly detached section with the block. The section may then be flattened on the block surface with brushes. There is no displacement to either side and no overhanging of section edges. The free end of the section, however, depending upon the degree of section compression, is more or less displaced from the adjacent end of the block.

Now, if the same block is sectioned with an oblique knife, and the section is similarly flattened, the section is both distorted and reoriented. Furthermore, relationships vary depending upon the angle of obliquity to which the knife is set. Figure 1 depicts the shape and extent of displacement of sections of the same thickness for knife sets of 15°, 30° and 45°, and a normal rake, in each case, of 55°. In all, the section outline is rhomboidal rather than rectangular as was the block face. The sections are wider than the block (greatest widths are associated with the 45° knife), and the long axis of the section is displaced laterally. For the 15° knife, displacement is to the left (away from the knife), while for the 30° and 45° knives, the sections slant to the right (or toward the knife) and this slant is more for the 45° than for the 30° knife.

Likewise, there is an increased compression in the axis of the knife movement as the knife angle is increased toward 45°. For knife angles greater than 45°, the amount of com-

pression decreases and approaches values dealt with in the study on the rotary microtome. Lateral displacement to the right becomes negligible at about 70°, and then begins a slight deviation to the left similar to that figured with the 15° knife. As the knife obliquity angle increases from 45° to 90° or decreases toward 0°, section width decreases to that of the original block. These effects are by no means limited to

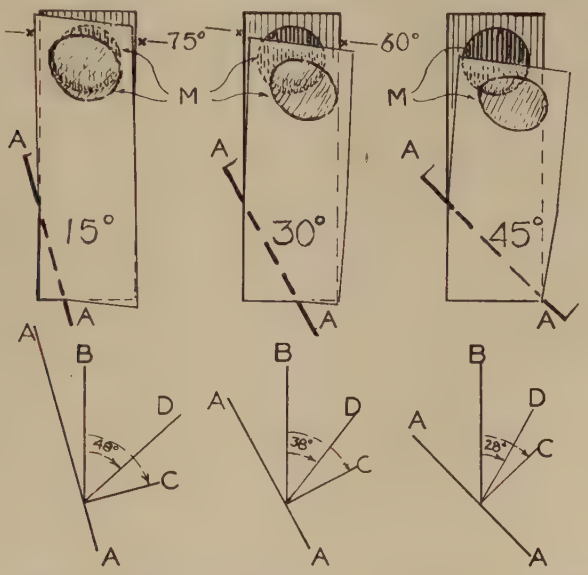

Fig. 1 The upper diagrams show distortions of sections by the sliding microtome for characteristic knife obliquities as indicated by A-A. "M" represents both the face of a cylinder of celloidin embedded in the block (vertical shading) and the distorted shape appearing in the section. Lines labeled 60° and 75° indicate the relative amount of section shortening in similarly shaped sections for 60° and 75° knife obliquity. Figures below show the significant axes involved in sectioning with the 15°, 30° and 45° knife. A-A = knife edge; B = axis of movement; C = cross sectional axis of knife; D = axis of compression.

paraffin sectioning; they may be shown with celloidin and in fact may be duplicated roughly with a hand plane and a block of soft wood such as pine or balsa.

Four effects thus appear as characteristic of the action of an oblique knife: (1) compression in the cutting axis which reaches a maximum for a 45° knife and then decreases to a

standard compression at 90°; (2) increased section width which also becomes maximal at 45°; (3) a lateral deviation of section axis toward the knife from about 20° to 70° (being maximal at 45°) and away from the knife for angles in the range 20° to 0° and 70° to 90°; and (4) increased section thickness to compensate for decreased section area. For thin sections, both lateral displacement and compression are greater than for thick sections.

In order to determine the direction of the axis of elongation (i.e., increased section width) and also the true compression axis, as contrasted with compression in the axis of knife movement, lathe-turned cylinders of paraffin infiltrated celloidin, colored, were re-embedded and sectioned. After such sections were flattened and affixed to glass plates, a magnified image of each was projected in an Edinger projector. The celloidin slice appeared as an elliptical or possibly egg-shaped area having perceptible parallel straight scorings due to microscopic imperfections of the knife edge. These scorings, also evident on the block surface with oblique illumination, corresponded with the direction of knife movement. By determining the major and minor axes of the ellipsoidal slices, it was possible to determine also the angles between these axes and the axis of knife movement. Thus, data were provided which could be visualized in terms of knife obliquity and direction of knife movement. The appearance of celloidin slices is represented on the diagrams already discussed (fig. 1 at M).

The smaller the knife angle, the farther was the axis of section compression displaced from the axis of knife movement. Conversely, as knife obliquity was increased toward 90° the axis of compression came closer to and finally, at 90°, coincided with the axis of knife movement. The axis of section elongation was, of course, 90° further removed. Elongation, when compared with compression, appeared to be of no great magnitude. In all cases, the compression axis is directed toward rather than away from the knife, and it falls between the axis of movement and the axis of knife cross section. Moreover, if the angle lying between the axis of movement

and the compression axis is compared with the angle between the axis of movement and the axis of maximum facet angle, a constant ratio obtains. For a knife so tilted that the upper facet makes an angle of 35° with the block face (i.e., normal rake of 55°), the former angle is close to 63.5% of the latter. These relationships, too, are diagrammed for 15°, 30° and 45° knife angles at the lower part of figure 1.

Though the amount of section shortening varies, as indicated above, with obliquity, a knife set at an angle of 20°, an angle commonly used, caused only a third the amount of compression of sections that was found with the rotary microtome (i.e., at similar section thickness and similar normal rake). Although compression was less, warping distortions, not possible with the rotary microtome, were present.

Except for the altered axes of distortion, the mechanics of section formation are the same for the oblique knife as for the transverse knife (preceding paper). Tissues are deformed like celloidin cylinders or like the paraffin itself, but the extent of deformation is ordinarily somewhat less than for the matrix material. The distortions, likewise, are permanent and may be significant in certain types of microscopy.

Correction of compression defects may be desirable in the making of drawings and plastic or graphic reconstructions. For sections from the rotary microtome, the one dimensional compression defect, if the increased section thickness is ignored, may be compensated for by: (1) transforming to a square system of coordinates, projection drawings made on a rectangular grid system with proportions corresponding with the gross distortion, (2) projection of the image of a section to an oblique drawing board and drawing the image as each level of the board is brought into focus, and (3) the use of appropriate cylinder lenses added to a projector. With a biaxial distortion in the plane of focus, however, as for sections from the sliding microtome, either the photographic method of Heard ('31), or the transference of a drawing from an appropriate rhomboidal grid system to a square system is required.

LITERATURE CITED

DEMPSTER, W. T. 1942 The mechanics of paraffin sectioning by the microtome. Anat. Rec., vol. 84, pp. 241–268.

———— Paraffin compression due to the rotary microtome. Stain Tech., vol. 18, (in press).

HEARD, O. O. 1931 A photographic method of orienting serial sections for reconstruction. Anat. Rec., vol. 49, pp. 59–70.

CHARACTERISTICS OF HUMAN SCHWANN CELLS IN VITRO

MARGARET R. MURRAY AND ARTHUR PURDY STOUT

Surgical Pathology Laboratory of the Columbia University College of Physicians and Surgeons and the Department of Surgery of the Presbyterian Hospital, New York

FOUR PLATES (TEN FIGURES)

In investigating the cellular origin of the specific nerve sheath tumor, or neurilemoma, the authors have employed the method of tissue culture, in the expectation that differences could be observed between the characteristics of the various components of the peripheral nerve. If the normal Schwann cell can be distinguished from the endoneurial or perineurial cell in vitro, where it can be seen as a whole and does not depend for identification upon its relationship to the nerve fiber or bundle, it should then be possible by cultivating the tumor in question to determine whether the cells which compose it come from one or the other of the neural elements. Such a procedure has a considerable chance of success providing the tumor cells are not greatly modified from the normal, as is usually the case in benign or slowly growing tumors. The application of this method to the neurilemoma (Murray and Stout, '40) has led us to conclude that this neoplasm arises from the Schwann sheath cell, rather than from either endoneurium or perineurium. This coincides with the views of Masson and of Nageotte, but differs from that advocated by Penfield ('32) and by the late F. B. Mallory ('14), who contended that since these tumors characteristically contain collagen and reticulin fibers they must arise from cells of mesoblastic origin, as endoneurium and perineurium were conceded to be. Masson ('32) and Nageotte ('32), though

accepting Harrison's demonstration that the Schwann cells of the peripheral nerves arise from neural crest, asserted that the longitudinal fibers and the Plenk-Laidlaw sheath of the neurilema were the products of the sheath cells themselves and not of the endoneurial cells. Their evidence has been accepted by some and questioned by others. Recently in a monograph on the benign and encapsulated tumors of the nerves Masson ('42) has adduced evidence, which if accepted will obviate further discussion of the potentialities of descendents of these two germ layers. In a study of the developing spinal nerves of 3–10 cm. human embryos, he derives both perineurium and endoneurium from the primitive sheath of Schwann, which envelops the elongating axones. Of the nerve trunk only the epineurium, then, remains as mesoblastic in origin, and this is not involved in discussions of the origin of the characteristic fibrous sheath of the axis cylinder.

In the present communication it is desired to describe briefly the form and behavior of cells from Schwann's sheath of normal human nerves cultivated in vitro. The material was derived from (1) a normal human embryo of 12 weeks gestation, obtained by hysterotomy in a therapeutic abortion; (2) normal human adult sympathetic ganglia and nerves, obtained at operation. In these cultures the cells of Schwann show a distinctive morphology and physiology which separate them from the other components of the nerve. Wallerian degeneration goes forward in vitro, thus making the identification of the sheath cell certain, wherever the alignment of the cells advancing out from the undisturbed nerve bundles does not do so. This is contrary to the report of Ingebrigtsen ('16), who cultivated sections of rabbit sciatic nerves, and obtained no growth in vitro unless the nerve had been sectioned and allowed to degenerate in vivo for at least 5 days before explantation. The descrepancy is probably traceable to improvements in the technique of tissue culture which have supervened in the interval since Ingebrigtsen's work was done. His cultures were simply incubated in plasma.

MATERIAL AND METHODS

From a human fetus of 12 weeks, the spinal nerves of the brachial and sciatic group were dissected out with fine forceps and scissors. The nerve trunk was loosened from its position against the body wall, and cut distally and proximally. These nerve sections were then examined microscopically to make sure that no fragments of skeletal muscle were adhering to them, and cut transversely into several pieces of a size suitable for explantation.

The adult material consisted of coeliac, splanchnic and lumbar ganglia with their associated nerve trunks, removed for various reasons from patients in their fourth and fifth decades. This material was cut in pieces, roughly 1–2 mm. on a side, and explanted.

The medium used for cultivation was a mixture of chicken plasma, extract of 9- to 11-day chick embryos in a buffered saline solution, serum ultra filtrate (prepared from beef blood by Dr. H. S. Simms), and human placental serum. The cultures were explanted in lying-drops of the medium according to the Maximow method and incubated at 37°C. They were washed in buffered saline three times a week, at which time the liquid components of the medium were renewed. The saline solution used was that devised by Simms and Sanders ('42). The cultures were maintained in their original situation on the flying coverslip, without transference, for as long as 1 month. During this time different explants were fixed, at intervals, in 10% formalin, Zenker's, Helly's, Bouin's, and Carnoy's fluids. They were stained with Delafield's hematoxylin, Mallory's phosphotungstic acid haematoxylin, fuchsin-ponceau-aniline blue, or, after fixation in formalin or Zenker's fluid, impregnated with silver by Foot and Mènard's modification of the Bielschowsky method, as adapted for tissue culture by McKinney ('29). For much of the technical work in both tissue culture and histology the authors are indebted to Miss Irene Bokoff.

OBSERVATIONS

Fetal Schwann cells

Within 2 days this material showed a growth whose nature appeared to be generally fibroblastic. In 4 or 5 days a new type of cell was apparent: a smaller, filamentous, bipolar cell, with a spindle or sausage-shaped nucleus containing one or two nucleoli (fig. 2). These could be traced emerging in tandem formation from the fasces of the nerve bundle. They were quite distinct from the background of fibroblasts against which they appeared. The latter were coarsely branching, often multipolar, and contained flattened oval nuclei with from two to seven nucleoli. When stained with fuchsin-ponceau or with Mallory's phosphotungstic acid hematoxylin, the sheath cells showed a cytoplasm that was relatively smooth and non-granular in texture, and more deeply staining than that of the fibroblasts. Though often single, these cells were likewise frequently joined to one another by their filaments, forming a thread dotted with nuclei. This habit is difficult to demonstrate in photographs because of the cells' tendency to meander through the clot.

At the 12-week stage of fetal development, differentiation and histogenesis are proceeding distally along these spinal nerves; so that one may come upon regions of nerves in which myelinogenesis is taking place. A favorably cut explant may show at one end a migration of sheath cells as described above, from unmyelinated fibers, and at the other end, after 8–10 days, a migration of much larger, multinucleate bodies from the myelinated portion of the fibers, in which Wallerian degeneration is taking place. It is not desired in this communication to give a detailed description of Wallerian degeneration per se; we shall hope to accomplish this in a later paper. In general, its course as we have observed it in vitro follows that charted by Nageotte ('22, '32); but in certain details it does not. For example, Nageotte states that the resolution of the myelin of the large medullated fibers is accomplished in vivo through the agency of wandering cells

of polyblastic nature, which are able to penetrate the sheath of Schwann and phagocytize the débris formed by the breaking up of myelin and axis cylinder after nerve section. In our cultures of fetal nerves this does not take place; the nerve is removed from its systemic relationships, and only such wandering cells as chanced to be present at the time of dissection can be included in the culture. These are negligible in numbers; the myelin (or pre-myelin) and axis cylinder are resolved within the Schwann cells which surround and enclose them. Figure 4 shows the situation at 10 days, in which digestion of the nerve fiber and its myelin are proceeding simultaneously with the migration of the Schwann sheath and the multiplication (probably amitotic) of its nuclei. The nuclei under these circumstances are more oval and less elongated than those described from the unmyelinated sheath, but they have the same complement of nucleoli; i.e. 1–2. The cell body is distended with globules of various sizes, some of which are colored by ponceau 2R, and others with aniline blue. Eventually all this material is digested and absorbed, and the sheath cell reverts to a ribbon-like or thread-like syncytium. At this stage of fetal development, longitudinal reticulin fibers are present in the nerve trunk; but the cell outgrowth in vitro is so mixed that it is impossible to determine the origin of such fibers as are found in it.

Adult Schwann cells from sympathetic nerves

The coeliac, splanchnic and lumbar ganglia and nerves which we have studied have been essentially similar. The ganglia themselves have contained aggregations of nerve cells, distinguishable in the explant by their lipochrome pigmentation, and nerve bundles passing in various directions. The extra-ganglionic portion of the coeliac and splanchnic nerves contained scattered ganglion cells, as well as nerve bundles roughly forming a trunk, all embedded in a tough connective tissue framework. It was not feasible to strip this connective tissue off from the nerve bundles, since the trauma resulting from such a procedure inhibits greatly, if not

entirely, the Schwannian growth. In the course of cultivation, many ganglion cells emigrated from the explants and disposed themselves in various formations through the plasma clot — a subject to be reported at a later date. The nerve bundles carried mainly fine medullated fibers and fibers of Remak. In these, as in the embryonic material, resolution of the contents of the Schwannian sheath was accomplished without benefit of phagocytes, though a few of the latter may be seen in contact with the exterior of the sheath cells in figure 5.

Within 3–5 days after explantation a brush of fine, filamentous processes could be seen emerging from the cut ends of the nerve bundles. By 6 or 7 days these had progressed to such an extent that their nuclei could be seen, as well as, in some cases, globules of myelin contained in the cell body close to the nucleus (fig. 7). Within 8–9 days the growth had become luxuriant and a few cells resembling fibroblasts were present in the medium. At 10 days ganglion cells could be distinguished, completely emerged from the explant. At 20 days, capillary buds were present in the outgrowth on some slides. The fibroblastic complement gradually increased.

The growth from the fibers of Remak, as might be expected, was finer than that from the unmyelinated fibers, and there was more of a tendency to side-branching. Figure 3 shows what appears to be longitudinal fission completed in the cytoplasm, and in progress through the nucleus (12 days). At 24 days one may find a situation such as is shown in figure 6, where the nuclear palisading which is characteristic of nerve sheath tumors and of Wagner-Meissner corpuscles is simulated in vitro by sheath cells from the fibers of Remak. This arrangement is apt to be transitory, probably because of the lack of compression in the cultures.

At the time of their emigration from the explant, the Schwann cells of the fine medullated fibers contain globules of myelin, and are often gnarled and coarsely branching, a condition which seems to be related to their content of débris. It does not interfere, however, with their basically bi-polar habitus. As cultivation is continued, and the débris is digested,

this pebbled appearance is lost, and a ribbon-like structure is produced, dotted with nuclei (fig. 5). These ribbons appear to thicken and to reproduce dichotomously (note the lateral filaments) and eventually to form structures akin to v. Bungner's bundles. The nuclei of Remak's sheath cells and those of the fine myelinated fibers are essentially similar: they are elongate, sometimes spindle-shaped, rather heavily dusted with fine chromatin particles, and provided with a small number of nucleoli — usually 1–3. Except when the cell body is distended with undigested débris, it usually bulges where the viscous, unflattened nucleus is located.

In a recent publication the authors have offered figures showing the development in vitro of reticulin fibers in areas occupied exclusively by Schwannian cells growing out from an intra-thoracic nerve sheath tumor originating inside the vertebral canal (Murray and Stout, '42). There the fibers formed more slowly and in a rather different pattern from those which developed, by comparison, in the stroma from a parathyroid adenoma cultivated in vitro under parallel conditions. The Schwannian reticulin fibers developed first singly, following the longitudinal axis of the cell and sometimes making a detour around the bulge of the nucleus; they did not appear first as a mat of fine criss-cross fibers as is the custom in connective tissue (Stearns, '41). We have since observed this same type of fiber development beside the Schwann cells emerging from a ganglioneuroma obtained from a 9-year-old girl and cultivated in vitro. Figure 8 shows the earliest form of longitudinal fiber development: a series of coalescing beads, or granules.

Figures 9 and 10 are from a normal splanchnic nerve cultivated for 28 days. The first shows a branching ribbon outlined in parts by longitudinal fibers, and an early bundle-formation in which the cloisonnement of which Masson ('42) speaks is beginning to appear. The second shows a bundle further advanced, in which the reticulin fibers closer to the explant are heavy and are beginning to be matted, while the distal fibers (formed later) are still single and rather fine. Capillary

formations which sometimes occur, and all cells of fibroblastic habit in the cultures have been carefully excluded from consideration in the above description of fiber formation; only Schwannian outgrowths in such a position and alignment that they could not be confused with other types of cells have been utilized.

DISCUSSION

It will be noted that the relationship between growth rates and latent periods of Schwann cells and fibroblastic components of the nerve seems to be reversed between the embryonic and adult material which we have described. Our general experience, in normal adult cultures, both human and animal, as well as in hyperplastic and neoplastic material, has been that the Schwann cell has a shorter lag period and a faster growth rate than the accompanying cells of fibroblastic nature. Nageotte and Masson also refer to this reproductive vigor which characterizes the adult Schwann cell, and which appears to be responsible for the "schwannoma" (Masson, '32) which is produced at the cut end of even the distal segment of a severed nerve. Ingebrigtsen ('16), in his cultivation of rabbit sciatic nerves in plasma alone reports a luxuriant growth of Schwann cells, and few fibroblasts. In the 12-week embryo which we have studied, however, the endoneurial and perineurial cells were definitely in the ascendency from the start, although during the period of cultivation they never completely overgrew the Schwann cells. It is possible that this reversal may be of a transitory nature and occurs only at this time, i.e., at the period when, according to Masson's account ('42), the endoneurium and perineurium are burgeoning from the primitive sheath of Schwann.

It has frequently been suggested in the literature that the Schwann cell of the peripheral nerves is similar in function to the oligodendrocyte of the central nervous system; indeed, among the French workers the sheath cell is often designated as "peripheral glia." Masson ('42), introduces the term "schwannoglia." In this connection it may be of interest to

mention a similarity in form between the fine, filamentous type of Schwann cell which was observed in our cultures of fetal nerves, and certain oligodendroglial cells photographed by Dr. Donal Murnaghan in cultures of embryonic mouse and chick spinal cord. (Personal communication from Doctor Murnaghan.)

Much has been written about the syncytial nature of the Schwann sheath, and of outgrowths from it in vivo and in vitro. Masson ('42) uses the term "symplasm" in describing it. It is evident from our material, both embryonic and adult, that Schwann cells are capable of separating themselves from the group and wandering off singly during the more differentiated stages of existence of the spinal nerves as well as in the early developmental stages, as described by Harrison ('24) and by Speidel ('32). In the outgrowths from the embryonic myelinated fibers, however, it is typical to find multinucleate structures (fig. 4), which are as unquestionably syncytial as skeletal muscle outgrowths at a corresponding period. The structures emerging from adult nerves are not so clear as to their intercellular relationships, and it has not been possible to investigate them by microdissection. But from observation of living and fixed material it appears that there is often longitudinal continuity between the units of cytoplasm extending on each side of a nucleus and those of adjacent nuclei; and in the outgrowths from the Remak fibers this continuity seems to include lateral anastomoses between longitudinal filaments. Ingebrigtsen likewise speaks of his outgrowths as syncytial.

Few mitoses have been observed among the Schwann cells of either embryonic or adult cultures. It is therefore difficult to avoid the conclusion that direct nuclear division takes place.

The formation of reticulin by normal adult Schwann cells has been demonstrated in these cultures. In view of the advances in the knowledge of organ and tissue lineage based on researches in experimental embryology over the last 20 years, it seems unnecessary to labor the point that cells

derived from one germ layer may form tissues and products which more typically characterize the descendents of another germ-layer. Raven's demonstration in 1931 that the mesectoderm of urodeles furnishes a part of the visceral skeleton provides a case sufficiently in point. It may be of interest, however, to note that the course of reticulin formation proceeds rather differently when engaged in by the Schwann cells than when the participants are fibrocytes. The product also is different: the longitudinal fibers and the Plenk-Laidlaw sheath of the neurilema form a highly specialized structure, of sharply circumscribed extent.

SUMMARY

The form and behavior in vitro of human Schwann cells from spinal nerves of a 12-week embryo are described, and compared with those from adult sympathetic ganglia and nerves. Minor differences and basic similarities are noted between the sheath cells of medullated and unmedullated fibers. Wallerian degeneration is shown to take place in vitro without a preliminary period of myelin disintegration in vivo, and without the intervention of phagocytes. Sheath cells are shown to form syncytial structures in vitro, as well as to exist singly. Their morphology is such as to distinguish them from endoneurial and perineurial cells as well as from the common and ubiquitous fibrocytes. In adult material their growth potency is markedly in advance of that of the other components of the peripheral nerves. Schwann cells from adult human sympathetic nerves have been shown to form reticulin fibers in vitro.

LITERATURE CITED

Harrison, R. G. 1924 Neuroblast versus sheath cell in the development of peripheral nerves. J. Comp. Neur., vol. 37, p. 123.

Ingebrigtsen, R. 1916 Contribution to the biology of the peripheral nerves in transplantation. J. Exp. Med., vol. 23, p. 251.

McKinney, R. L. 1929 Studies on fibers in tissue cultures. III. The development of reticulum into collagenous fibers in cultures of adult rabbit lymph nodes. Arch. f. exper. Zellforsch., vol. 9, p. 14.

MALLORY, F. B. 1914 The Principles of Pathologic Histology. W. B. Saunders & Co., Philadelphia, Pa.

MASSON, P. 1932 Experimental and spontaneous schwannomas (peripheral gliomas). Am. J. Path., vol. 8, p. 367.

———— 1942 Tumeurs encapsulées et bénignes des nerfs. Revue canadienne de Biologie, vol. 1, p. 209.

MURRAY, M. R., AND A. P. STOUT 1940 Schwann cell versus fibroblast as the origin of the specific nerve sheath tumor. Am. J. Path., vol. 16, p. 41.

———— 1942 Demonstration of the formation of reticulin by Schwannian cells in vitro. Am. J. Path., vol. 18, p. 585.

NAGEOTTE, J. 1922 L'organisation de la matière dans ses rapports avec la vie. Etudes d'anatomie générale et de morphologie expérimentale sur le tissu conjonctif et le nerf. Librairie Félix Alcan, Paris.

———— 1932 Sheaths of the peripheral nerves. Nerve degeneration and regeneration. Cytology and Cellular Pathology of the Nervous System, Penfield, Wilder, Ed. Paul B. Hoeber, Inc., New York.

PENFIELD, W. 1932 Tumors of the sheaths of the nervous system. Cytology and Cellular Pathology of the Nervous System, Penfield, W., Ed. Paul B. Hoeber, Inc., New York.

RAVEN, C. P. 1931 Zur Entwicklung der Ganglionleiste. 1. Die Kinematik der Ganglionleistentwicklung bei den Urodelen. Arch. f. Entwicklungsmechanik, vol. 125, pp. 210–292.

SIMMS, H. S., AND M. SANDERS 1942 The use of serum ultra-filtrate in tissue cultures for studying fat deposition and for virus-propagation. Arch. Path., vol. 33, p. 619.

SPEIDEL, C. C. 1932 Studies of living nerves. I. The movements of individual sheath cells and nerve sprouts correlated with the process of myelin sheath formation in amphibian larvae. J. Exp. Zool., vol. 61, p. 279.

STEARNS, M. L. 1940 Studies on the development of connective tissue in transparent chambers in the rabbit's ear. Am. J. Anat., vol. 66, p. 133.

PLATE 1

EXPLANATION OF FIGURES

1 Schwannian outgrowth from medullated fibers of a spinal nerve from a 12-week human fetus. Ten days in vitro. Bouin; acid fuchsin, ponceau, aniline blue.

2 Schwannian and endoneurial outgrowth from unmyelinated portion of a spinal nerve, from a human fetus, 12 weeks. Ten days in vitro. Zenker, phosphotungstic acid haematoxylin. *S*, Schwann cell. *E*, endoneurium.

1
S
S
E
2

PLATE 2

EXPLANATION OF FIGURES

3 Schwannian filaments from fibers of Remak of a human adult coeliac nerve. Twelve days in vitro; formalin, Delafield's haematoxylin.

4 Outgrowth of sheath cells from medullated fibers, showing Wallerian degeneration and syncytial structure. Human fetus, 12 weeks, spinal nerve. Ten days in vitro. Bouin, acid fuchsin, ponceau, aniline blue.

5 Outgrowth from fine myelinated fibers, human adult coeliac nerve. Twenty-four days in vitro. Carnoy, Delafield's haematoxylin. *P*, phagocyte.

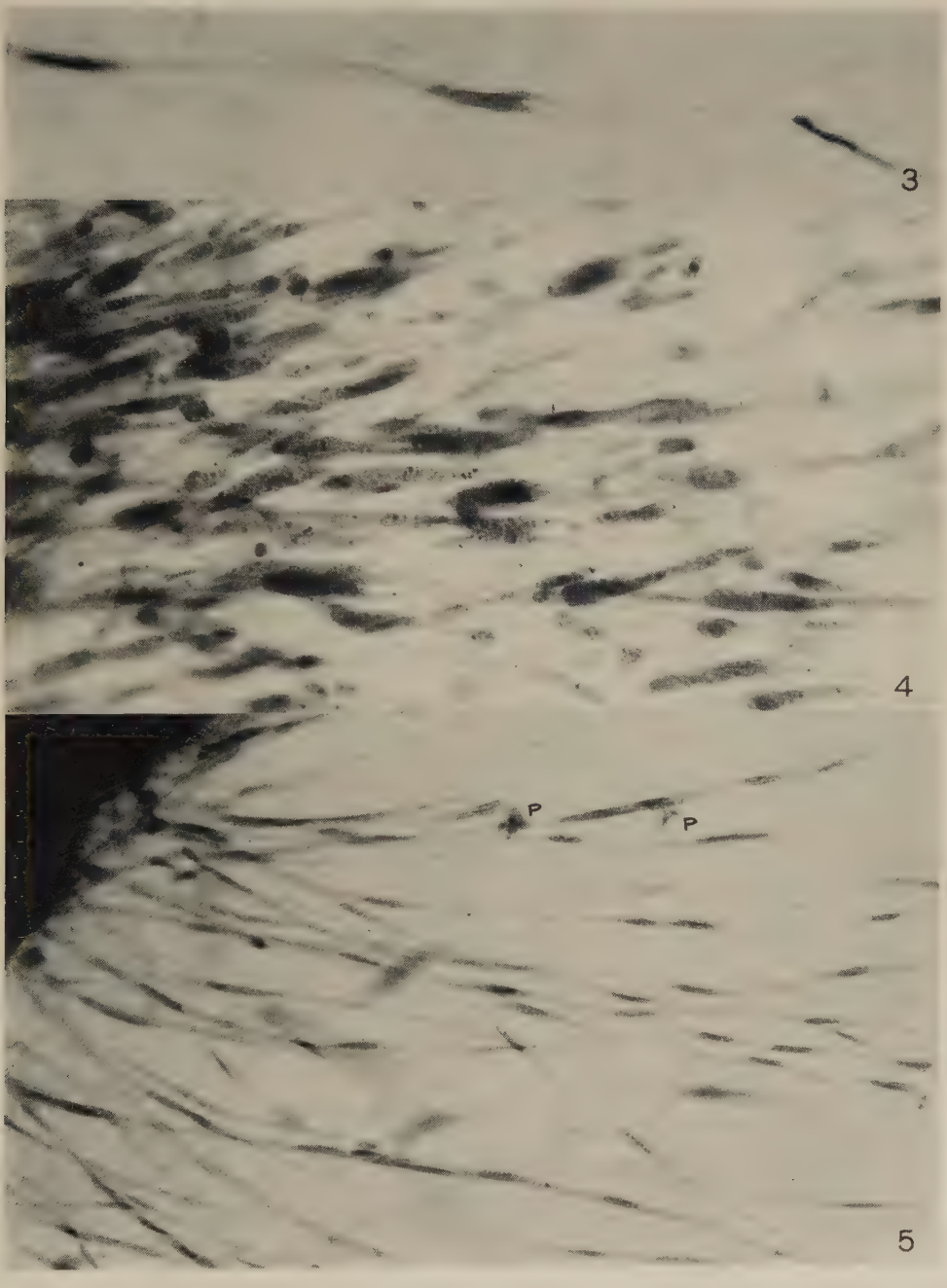
3
4
P
P
5

PLATE 3

EXPLANATION OF FIGURES

6 Outgrowth from fibers of Remak, human adult coeliac nerve. Twenty-four days in vitro. Carnoy, Delafield's haematoxylin.

7 Schwann cell from fine medullated fiber, human adult coeliac nerve. Twelve days in vitro. Formalin, Delafield's haematoxylin.

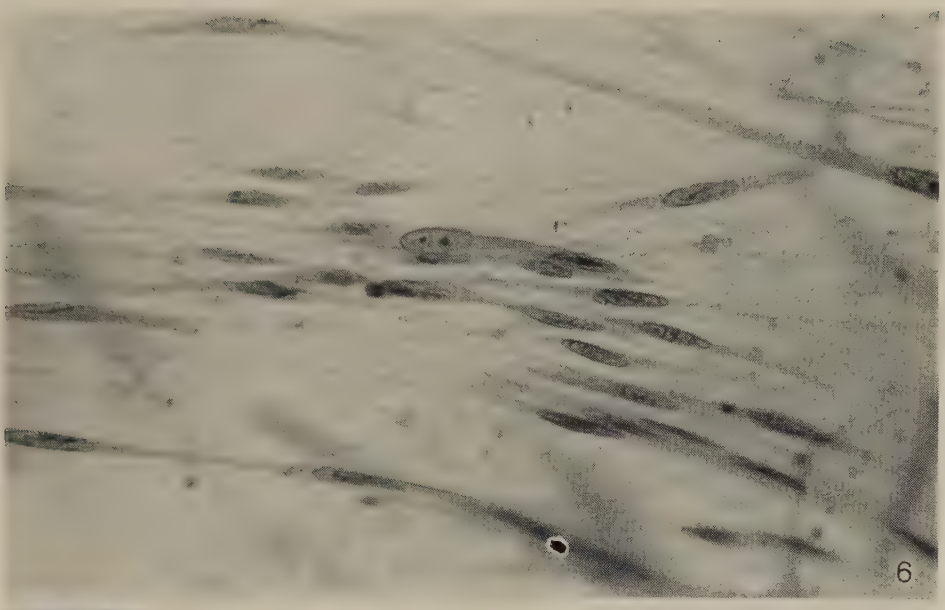
6

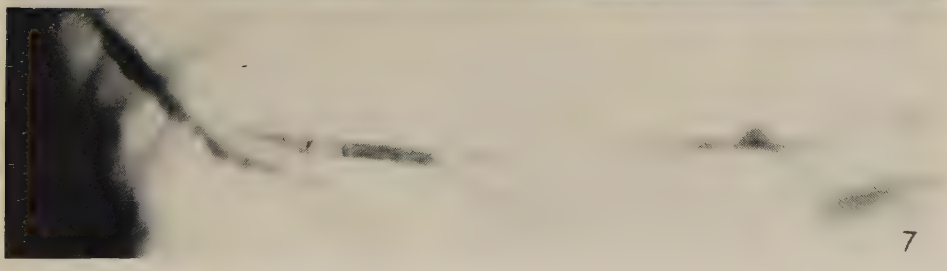
7

PLATE 4

EXPLANATION OF FIGURES

8 Early stage of reticulin formation around Schwann cell from ganglion-neuroma. Twenty-one days in vitro. Formalin, Foot's silver impregnation. *R*, beads of reticulin.

9 Schwannian ribbons from greater right splanchnic nerve of human adult. Twenty-eight days in vitro. Formalin, Foot's silver impregnation. *L*, longitudinal fiber; *C*, cloisonnement.

10 Further advanced reticulin formation from same specimen as above. Twenty eight days in vitro. Formalin, Foot's silver impregnation. *M*, secondary matting of fibers; *L*, fine longitudinal fibers. This photograph was taken at two focal levels, and the two halves joined in the middle.

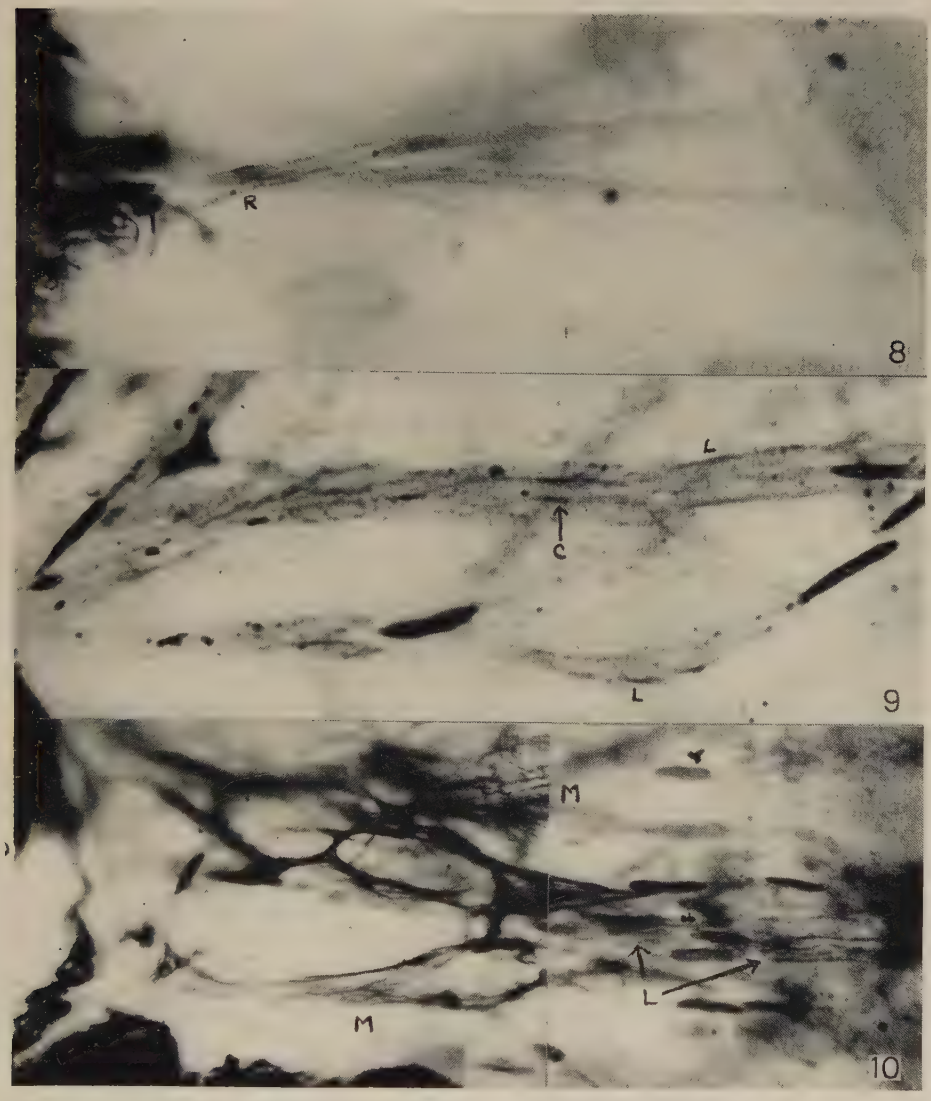
R
8
L
C
L
9
M
L
M
10

THE SCLEROTIC PLATES OF THE WHITE LEGHORN CHICKEN[1]

NORMAN M. NELSON
U. S. Regional Poultry Research Laboratory, East Lansing, Michigan

THREE FIGURES

In a study of the physiological anatomy of the avian eye as a basis for an elucidation of the disease, ocular lymphomatosis, certain interesting structural features were observed and are described in this paper.

The eyes of birds, as well as eyes of other species of animals, contain a bony ring at the corneal-scleral junction. Moy-Thomas ('41) referred to these bones in the fish as the "dermal bones." The use of the term "dermal bones" apparently is based upon the osteogenesis of the skull. Murray ('41), referring to the fowl, called them the "dermal bones of the sclerotic." Slonaker's ('18) terminology was either "scleral bones" or "scleral plates," and Chard and Gundlach ('37) followed Slonaker in the use of these terms. Bradley ('38) mentioned that the sclera of the chicken eye contains a bony scleral ring.

Murray ('41) stated: "It is well known that the fowl has fourteen dermal bones in its sclerotic, forming a ring around the pupil." He did not mention an irregularity as to number or arrangement. Murray allied the epidermal papillae of the conjunctiva of the 7-day embryo as concerned with the development of the scleral bones. Lillie ('40) described the epidermal papillae referring to them as "papillae conjunctivae sclerae" but did not associate their presence with the later development of the scleral plates.

[1] This paper is a portion of the thesis in partial fulfillment of the requirements for the Ph.D. in Animal Pathology, Michigan State College.

Slonaker stated that the number, size, and arrangement of the plates vary in different species of birds. He did not indicate a variability of number or arrangement within a species but described the overlapping as regular and shingle-like in arrangement in the English sparrow (Passer domesticus). Chard and Gundlach ('37) found that the number of plates in the homing pigeon was "about ten." This may indicate that these writers did observe a variability in the number of plates.

The sclera or sclerotica is the dense, opaque, fibrous portion of the eyewall. In the fowl the sclera is cartilaginous except at the anterior limit where the bony scleral plates occur and at the point of entrance of the optic nerve where the os opticus is found in some birds.

This paper concerns only the scleral ring and will not consider the os opticus, the u-shaped bone of the avian sclera which surrounds the optic nerve entrance as described by Tiemeier ('39). The scleral ring and the os opticus are distinctly two separate anatomical features. As Tiemeier pointed out, the os opticus has been referred to as "the rear sclerotic ring." He stated that the os opticus may be differentiated from the scleral ring microscopically by the marrow cavity which it contains. The scleral plates which make up the sclerotic ring are solid bone. Tiemeier quoted Leydig (1855) as stating that the sclerotic ring is formed by calcification of connective tissue, while the os opticus is formed by calcification of the hyaline cartilage of the sclera.

MATERIALS AND METHODS

Rings from eyes of fifty pedigreed Single-Comb White Leghorn birds were examined. For the most part, these were unselected cases, although in some instances several were saved from a single family. In all, the fifty birds represented twenty-eight families. (A family is represented by the progeny of a mating of a single selected male and female.) There were seventeen males and thirty-three females. These fifty birds were from 8 to 33 months of age. In addition, a

small number of eye rings from 18-day-old embryos were examined.

Various technics were used for exposing the plates, but a simple and satisfactory method was simply to scrape the fibrous tissue off the external surface with a small scalpel after bisecting the globe just posterior to the outer limit of the scleral ring. A low power binocular was used for this dissection. The eyes were first removed from the head and the position in the head was marked at the dorsal side by puncturing the cornea. The anterior portion (external wall) was then excised. By leaving the fibrous tissue attached to the medial side, the plates were held together and the ring, its component plates, and their arrangement could then be examined.

MORPHOLOGY OF THE PLATES AND RING

The sclerotic plates of the chicken are embedded in the fibrous portion of the sclera, encircle the limbus, and are thus in close proximity to the cornea at the inside circumference border. The outside circumference border overlaps the cartilaginous layer of the sclera. The eye globe of the domestic fowl may be described as a flattened sphere. Thus the sclerotic plates and the cornea make up the external eye wall and in this way, form a lid for the cup-shaped globe. Individual plates are not flat but are curved outwardly on the inside border adjacent to the limbus. On cross section the shape is sigmoid or similar to the diacritical sign, the tilde (~), (fig. 1). In this way a flange or hub-like projection is formed by the inside border of the ring. On the external surface a fibrous band encircles the hub, thus adding strength to the mechanism, without interfering greatly with slight motility. Attached to each plate are radial fibers which at their outer limits become a part of the fibrous layer of the sclera. The medial flat surface is covered by a less dense fibrous layer which serves in part as an anchor for the ciliary muscles.

The ring formed by the plates is nearly circular in appearance, compressed slightly on either side parallel to the vertical axis. The ring appears asymmetrical because the plates on the nasal side are narrow and long, while on the

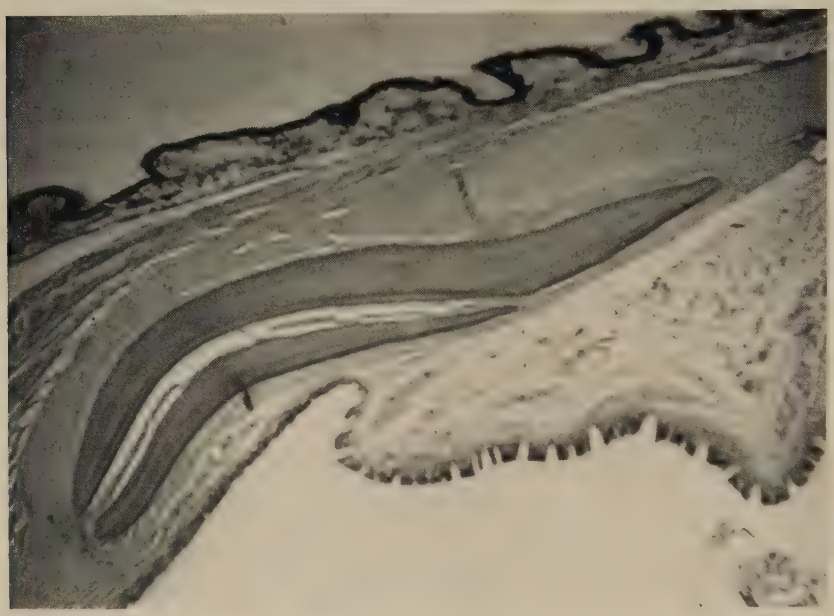

Fig. 1 Cross section of the scleral plates. (The limbus area is at the extreme lower left and the cartilaginous layer of the sclera can be seen at the right.)

lateral or temporal side they are shorter and wider (fig. 2). This increased width on the temporal side builds out the hub on that side, and in this way may materially increase the angle of binocular vision, as well as give greater protection to the eye on that side.

The plates are roughly quadrilateral in outline with somewhat rounded corners. A single plate is thickest in its centrium, gradually tapering off to the borders.

The size of individual plates is dependent on the size of the bird. In a mature female fourteen plates averaged 4.34 mm. in length and 2.62 mm. in width. The longest plate was 5 mm. in length by 2.1 mm. in width, whereas the shortest plate was

4 mm. in length and 3.1 mm. in width. Thus a difference of 1 mm. in dimensions each way was observed. The long narrow plates were always adjacent to the nasal canthus and consistently overlapped in the same direction. Each plate, with

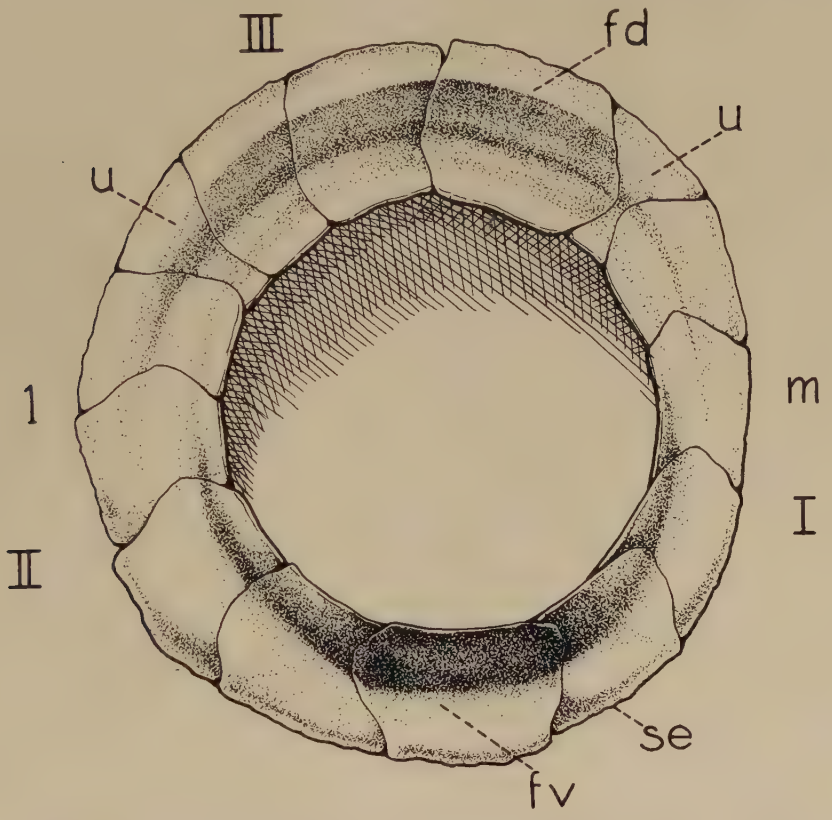

Fig. 2 Drawing of the scleral ring from the right eye of a hen, showing asymmetry of the circle, overlapping design of type A. (I, II, III designate grouping of plates as to directional overlapping; f.v., front ventral plate; f.d., front dorsal plate; u., underlapping plate; m., medial side; l., lateral side; s.e., serrated outer edge. Approximately × 7.)

certain exceptions which will be described later, overlaps the adjacent plate approximately one-third of its length. Thus the thickness of the two combined tapered portions about equals the thickness of the plate at its center. A ring, fairly uniform

in thickness, is thus formed, completely surrounding the limbus.

The combination of the scleral plates, the fibrous layers, and cartilaginous portion of the sclerotica gives a remarkable reinforcement to the globe. Due to the large size of the eye in the bird in relation to the size of the head, such a protection is obviously advantageous. There are other structural adnexa such as the membrana nictitans of the eyes of certain amphibia, reptilia, and aves which are primarily protective features. In the bird the medial sides of the posterior walls of the eyes are separated only by an osseus septum, and the lateral or external walls protrude from the orbit. The lacrimal and frontal bones form the antero-dorsal border of the bony orbit. This border is extended by a fibrous sheath in the domestic fowl. In this way the globe gains added protection not afforded by the skull. For protection of the inner eye, the external anatomical milieu would be inadequate without the reinforcement of the sclerotica by the bony plates.

NUMBER OF PLATES

Scleral rings from a given bird did not always have the same number of plates in both rings. Forty pairs of rings were constant in number with fourteen plates in each eye. One pair had fifteen plates in either eye and the individual rings

TABLE 1

Variation in number and arrangement of plates according to pairs of eyes in fifty chickens.

Number of pairs, 14 plates in either eye	40
Number of pairs, 15 plates in either eye	1
Number of pairs of unequal numbers	9
Number of pairs, same arrangement in both eyes	30
Number of pairs, different arrangement in either eye	20

of nine pairs were unequal in number of plates (tables 1 and 2). Thus it is apparent that the ring structure in these instances was variable in number and therefore asymmetrical in design. In considering the 100 rings individually, eighty-

eight rings contained fourteen plates each, eight rings contained fifteen plates each, and in addition there were two rings with thirteen plates each, and two rings with sixteen plates each. When more than fourteen plates were found, the additional plates were shorter in length than the average, in some cases being equal in length and width.

TABLE 2

Variation in number of sclerotic plates in nine pairs of eyes.

NO. OF PAIRS	NO. OF PLATES	
	Right eye	Left eye
1	16	14
2	15	14
3	14	15
1	13	14
1	14	13
1	15	16

TYPES OF ARRANGEMENT

A classification of the various arrangements was readily established by the well-defined designs as marked by the overlapping of the plates. Certain deviations did occur, however, in some of the rings which required placing them in the group which they most nearly resembled (fig. 3).

It will be observed in type A, there are three groups of plates, as marked by their direction of overlapping (I, II and III). The group on the nasal side has been designated as group I inasmuch as the number of plates and direction of overlapping were quite constant. Only one exception involving group I was found and this was classified as type D. In this series of four plates a given plate always overlapped the adjacent plate just dorsal to it. Group II likewise contained four plates but these overlapped with the opposite ends from those in group I. The two groups were divided by a single plate which overlapped both adjacent plates and was, therefore, designated as the front ventral plate. A third series of two plates overlapped similarly to group I but was separated from group I by a front dorsal plate which over-

lapped both adjacent plates. These overlapping or dorsal plates occurred between groups I and III and between groups I and II (fig. 3, A). In seventy-four of the 100 single rings, the plates were arranged as type A.

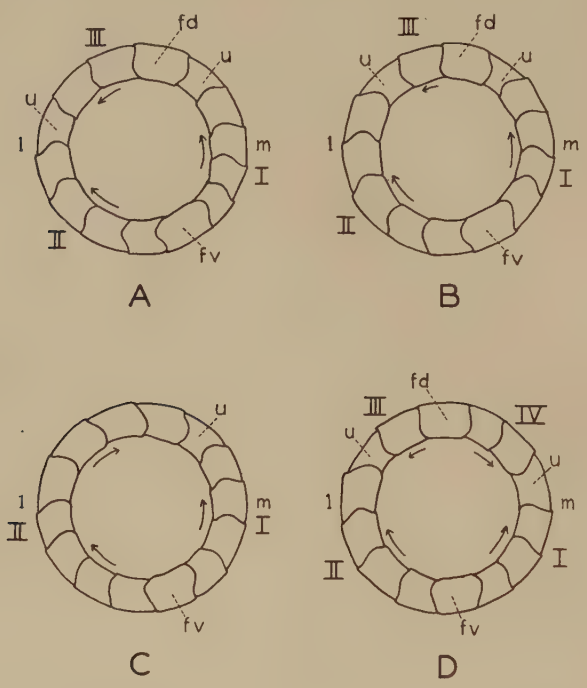

Fig. 3 Outline drawing of scleral rings, external view showing types of arrangement in right eyes. (I, II, III, IV refer to the groups of plates as demonstrated by the overlapping; l., lateral side; m., medial side; f.v., front ventral plate; f.d., front dorsal plate; u., underlapping plate. The arrows indicate the direction of overlapping.)

Type B differed from type A only in that group II contained five plates and had only one plate in group III. Type B occurred in twenty single rings. In type C the front dorsal plate was not recognizable, and the II group was continued and contained eight plates. Type C arrangement was found in five single rings, but did not occur in a symmetrical pair. In type D group I contained a series of only three plates; the

II group, a series of four plates; group III only one; and a fourth group occurred on the top medial side containing two plates. However, this arrangement, type D, was found in the ring of a single eye.

Inasmuch as the type A arrangement was found in seventy-four rings of 100 eyes, it was considered the most regular arrangement (table 3). Of the fifty pairs, both eye rings

TABLE 3

Arrangement types of sclerotic plates in paired and single eyes.

ARRANGEMENT TYPE	NO. OF PAIRS (SAME ARRANGEMENT IN BOTH EYES)	NUMBER OF SINGLE RINGS
A	28	74
B	2	20
C	0	5
D	0	1

TABLE 4

Variation in arrangement types of plates occurring in twenty paired eyes.

	NUMBER
Type A and B	14
Type A and C	3
Type A and D	1
Type B and C	2
Type B and D	0
Type C and D	0

had the same arrangement in thirty pairs, whereas in the remaining twenty pairs, various combinations occurred (table 4).

Forty-seven rings showed slight deviations in either of type A, B, or C. These irregularities consisted of incomplete over or underlapping of plate edges. This incomplete overlapping by one plate occurred most frequently in the front dorsal plate, but occasionally one of the plates of group II or III demonstrated the irregularity.

DISCUSSION

Variation in number and arrangement of sclerotic plates within a breed of a single species has been identified. Examina-

tion of embryos revealed that the plates are formed during embryonic development and the thin edges have overlapped by the end of incubation period. Thus it is possible that the relative head position of the embryo at the time the plates come in apposition may account for some of the variation in the arrangement of these plates, and the slight deviations may be due to pressure from some movable part. This would not, of course, explain the variation of difference in numbers of plates. The number of plates could not be identified as a family trait although the number of sibs examined was admittedly too small for a genetic study. Due to the variation of arrangement and number of plates in the two rings of a given bird, a large number of combinations would be encountered in a genetic study. Such a study should necessarily involve a large number of sibs from several families.

Slonaker believer that the primary function of the scleral plates had to do with accommodation. He stated that in sections of different eyes, different degrees of bending were observed. This observation would appear to be insufficient evidence as to their function, as the degree of curvature would naturally vary in sections taken at different angles, or indeed, because of the shrinkage in fixation. Slonaker himself illustrated the effect of the stress placed upon the tissues by the hardening fluids. He indicated that the bones furnished elasticity to the front of the eye which tended to restore the cornea to its original shape when the ciliary muscles were relaxed during focusing on distant objects. By the increase in intraocular pressure produced by the ciliary muscles pulling on the scleral walls, an increased curvature of the cornea would be produced, allowing the eye to focus on near objects. Chard and Gundlach subscribed to this belief.

Had the arrangement been identical in all eyes, an explanation might have been advanced on the effect of stress applied by the ciliary muscles at different points in the circumference of the scleral ring. If Slonaker's theory of accommodation in the bird is correct, it might be suggested that during domestication the chicken has lost the power of

rapid accommodation because of the irregular physiological structure of the sclerotic rings. Wood ('17) considered the absence of the fovea centralis in the chicken as evidence of decreased visual acuity and this evolutionary change he believed was due to domestication.

It would seem that the function of the scleral plates in the present-day domestic fowl is primarily one of protection to the eye globe. They are essential for this purpose because of the large size of the eye for the relative size and shape of the head. The surrounding soft tissues medial to the eye are in themselves inadequate in their protective influence. A definite arrangement of the plates in the wild bird may have assisted in rapid accommodation.

SUMMARY

The scleral plates of the White Leghorn chicken (Gallus domesticus) have been described. Variation in the number and arrangement of the plates in the 100 rings examined has been reported. It is suggested that the variability of arrangement may be due to embryo movement at the time the thin plate edges are large enough to begin over-lapping. The variation in number of plates is suggestive of genetic influence but no correlation was found in the family groups examined. The function of the plates is believed to be primarily one of protection in the present-day domestic fowl. The scleral plates have not been found affected in osteopetrosis.

The author acknowledges the preparation of the drawings to Miss A. Rudolphi of Detroit, Michigan.

LITERATURE CITED

Bradley, O. Charnock 1938 The structure of the fowl. 2nd edition, Oliver and Boyd, London.

Chard, Roy D., and Ralph H. Gundlach 1937 The structure of the eye of the homing pigeon. J. Comp. Psychol., vol. 25, pp. 249–272.

Leydig, F. 1855 Der hinter schlerotikalring im auge der Vögel. Müllers Archives für Anatomie 1855, pp. 40–46. (Cited by Tiemeier, '39.)

Lillie, Frank R. 1940 The development of the chick. Henry Holt and Company, New York.

Moy-Thomas, J. A. 1941 Development of the frontal bone of the rainbow trout. Nature (London), vol. 147, pp. 680–681.

Murray, P. D. F. 1941 Epidermal papillae and dermal bones of the chick sclerotic. Nature (London), vol. 148, p. 471.

Slonaker, James Rollin 1918 A physiological study of the eye and its accessory parts of the English sparrow (Passer domesticus). J. Morph., vol. 31, pp. 351–459.

Tiemeier, Otto W. 1939 A preliminary report on the os opticus of the bird's eye. Zoologica (N. Y.), vol. 24, pp. 333–338.

Wood, Casey Albert 1917 The fundus oculi of birds. The Lakeside Press. Chicago.

THE BLASTOCYST OF THE MARTEN (MARTES)

WILLIAM H. MARSHALL AND ROBERT K. ENDERS
Fish and Wildlife Service, United States Department of the Interior, Washington, D. C., and Edward Martin Biological Laboratory, Swarthmore College, Pennsylvania

TWO FIGURES

In his review "Delayed Implantation and Discontinuous Development in Mammals" Hamlett ('35) states that two families and six genera of Carnivora apparently show this phenomenon but that definite embryological proof was available for the badgers only. In a recent paper Wright ('42) offers the proof confirming Hamlett's suggestion that in the marten (Martes americana) and other American martens delayed implantation accounts for the long gestation period in this mustelid. To the records published by Wright we can add observations on seventeen unimplanted blastocysts from eight marten (Martes caurina caurina) collected in the winter months. For a discussion of the breeding season, length of the period of gestation and bibliography the reader is referred to Hamlett's and Wright's papers.

MATERIALS AND METHODS

In the past 3 years the senior author has spent much time studying the marten in the wild in Idaho. In this study trappers cooperated by saving fresh carcasses of the western pine marten (Martes caurina caurina) that had been taken for fur. The reproductive tracts of all females received in good condition were removed and preserved in 10% formalin. All ovaries were sectioned serially and stained. Where corpora lutea were present the uterus was sectioned too. Skulls were saved in order to determine the age of each individual. Table 1 lists the date the animals were caught, the

number of corpora lutea in each ovary, the number of blastocysts found and, wherever preservation was sufficiently satisfactory, the number of cells in each inner cell mass. Thanks are due to O. P. Pearson and D. W. Bishop for preparing the material and for aid in making cell counts, etc.

TABLE 1

ANIMAL NO.	DATE	NUMBER OF CORPORA	NUMBER OF BLASTOCYSTS	INNER CELL MASS
108	10/20	1 — 1	1	393
107	10/20	1 — 1	2	388, 362
156	10/23	2 — 1	3	391, 318, 174
153	12/5	2 — 1	3	368
166	1/19	2 — 1	1	363
42	Jan.	2 — 0	2	313
54	Jan.	2 — 1	3	325
139	Jan.	1 — 1	2	589, 508
162	2/19	2 — 1	3	Poor preservation

Fig. 1 Drawing of blastocyst. October 20. × 120.

DESCRIPTION

The zona pellucida is very conspicuous but no detail of its structure is visible in this material. In some blastocysts the sub-zonal cells can be distinguished chiefly by their nuclei, for the cell bodies are much attenuated as though the blastocyst had expanded rapidly. In others the cell bodies lie in crypts formed in the zona. Projections of the zona may be formed by these crypts; otherwise the zona is smooth. A coagulum is

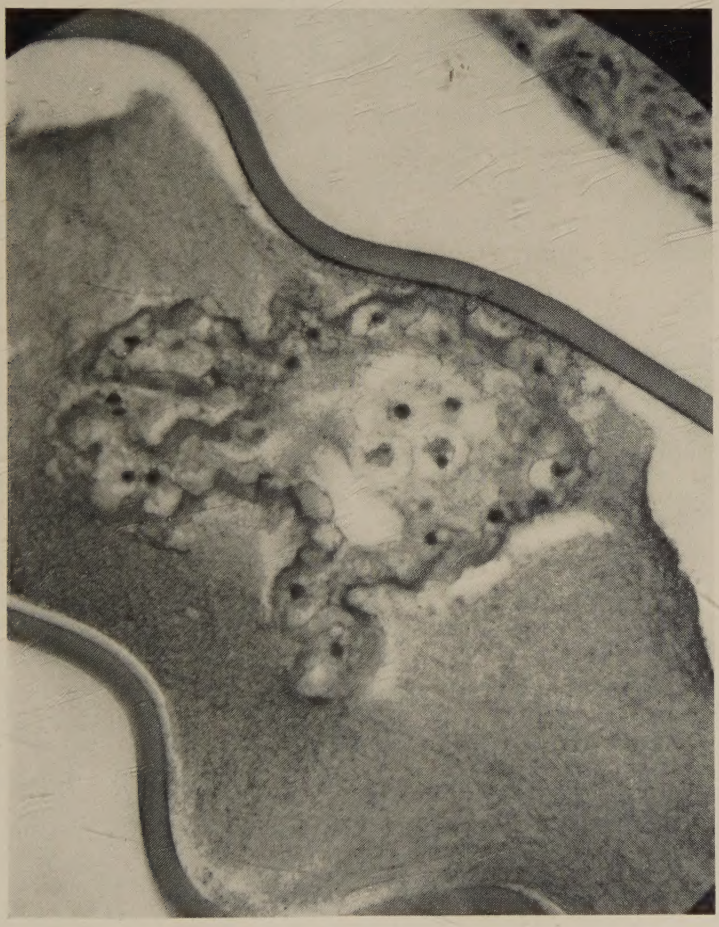

Fig. 2 Inner cell mass. January. × 510.

present within the cavity. The great irregularity of the blastocysts leads one to believe that they collapsed either before or during preservation. This same irregularity makes it difficult to determine the diameter with any degree of accuracy; this lies somewhere between .5 and .9 mm. which is rather small compared with the badger. The date in January on which no. 139 was killed is not known. This is regrettable for inner cell masses contained 508 and 589 cells, a possible indication that the blastocysts were becoming active. All of the other blastocysts excepting one of three recovered from no. 156 contained inner cell masses of from 313 to 393 cells. No explanation of the small mass in the one blastocyst of no. 156 can be advanced. Taking the average figure the inner cell mass contains approximately six times as many cells as that of the American badger during December, January and the early part of February (Hamlett, '32, p. 288). The inner cell masses are very irregular in outline and were not measured.

SUMMARY

Unimplanted blastocysts have been found in the uteri of the Western pine marten (Martes caurina caurina) killed in October, November, December and January. The inner cell mass of the blastocyst contains approximately 300 to 400 cells, the variation being from 174 to 589.

LITERATURE CITED

HAMLETT, G. W. D. 1932 Observations on the embryology of the badger. Anat. Rec., vol. 53, pp. 283–303.

———— 1935 Delayed implantation and discontinuous development in the mammals. Quarterly Review of Biology, vol. 10, pp. 432–447.

WRIGHT, PHILIP L. 1942 Delayed implantation in the long-tailed weasel (Mustela frenata), the short-tailed weasel (Mustela cicognani), and the marten (Martes americana). Anat. Rec., vol. 83, pp. 341–349.